CONFORMATIONAL ANALYSIS OF 2-SUBSTITUTED CYCLOHEXANONE KETAL DERIVATIVES BY MOLECULAR MECHANICS AND NUCLEAR MAGNETIC RESONANCE

by

TEREZA VARNALI

B.S. in Chem., Boğaziçi University 1979
M.S. in Chem., Boğaziçi University 1982

Submitted to the Institute for Graduate Studies in Science and Engineering in partial fulfillment of the requirements for the degree of

Doctor
of
Philosophy

Boğaziçi University
1986

ACKNOWLEDGEMENTS

I wish to acknowledge my sincere gratitude to Doç.Dr. Hadi Özbal for his most valuable advice and guidance without which this study could not have been completed.

I would like to express my sincere appreciation to Doç.Dr.Belkıs Halfon, Prof.Dr.Yüksel İnel and Doç.Dr.Sevil Öksüz for their careful and constructive review of the final manuscript and to all other members of the faculty for their valuable comments and helpful suggestions.

I am indepted to Gülnur Elöve from Villanova University for her kindly assistance in the recording of 200 MHz ^{1}H-NMR spectra.

Finally, I wish to thank my husband without whose support, understanding and encouragement it would not have been possible to devote the time and effort required for completing this study.

DEDICATION

TO

My husband Davit

My son Kaan

and

My Parents

CONFORMATIONAL ANALYSIS OF 2-SUBSTITUTED CYCLOHEXANONE KETAL DERIVATIVES BY MOLECULAR MECHANICS AND NUCLEAR MAGNETIC RESONANCE

The present study is concerned with the application of the Molecular Mechanics Method to 2-substituted cyclohexanone ketals. The object is to find the conformational free energy difference between the equilibrating conformers and to compare the theoretical results to those found experimentally.

For the application of molecular mechanics, models of the compounds under investigation were described, the interatomic distances and angles were computed, the most important interactions were determined and the parameters needed for calculations of the interactions and functions relating parameters to energy were chosen.

First, molecular mechanics was applied to spiro-[5,4]-1-halo-6,9-dioxodecane (1 in Fig.1.1.1) and spiro-[5,5]-1-halo-6,10-dioxoundecane (2 in Fig.1.1.1) where the halogen was chlorine or bromine. The results obtained theoretically showed preference for the conformer bearing the axial halogen in (2) system and the conformer bearing the equational halogen in (1) system, being in accordance to experimental results reported by Zefirov et. al.

Secondly, molecular mechanics was applied to spiro-

[5,4]-1-nitro-6,9-dioxodecane and spiro-[5,5]-1-nitro-6,10-undecane and the results obtained theoretically in contrast to halogens, showed preference for the conformation in which the nitro group is equatorial in both cases (1) and (2).

Finally, the 4-t-butyl derivatives of the nitro-(1) and (2) systems, and the (1) and (2) systems were synthesized and the free energy difference between the equilibrating conformers were obtained experimentally using NMR parameters. Experimental results were in parallel to those found theoretically.

In previous studies the nitro group has been shown to behave differently than halogens and similar groups due to its electronic distribution, size, structure and formal charge. The unique behavior of the nitro group has been shown once more both theoretically and experimentally.

2-SÜBSTİTÜE SİKLOHEKSAN KETAL TÜREVLERİNİN MOLEKÜLER MEKANİK VE NÜKLEER MANYETİK RESONANS İLE KONFORMASYONEL ANALİZİ

Bu çalışmada 2-sübstitüe sikloheksanon ketal'lerine Moleküler Mekanik metodu uygulanmıştır. Amaç halka çevrilmesi ile dengede bulunan iki konformerin arasındaki serbest enerji farkını hesaplayıp sonuçları deneysel sonuçlarla karşılaştırmaktır.

Moleküler Mekanik Metodunun uygulanabilmesi için önce modeller tasvir edilmiş, atomlar arası mesafe ve açılar hesaplanmış, önemli etkileşimler ve bu etkileşimleri enerji cinsinden tarif eden fonksiyon ve parametreler saptanmıştır.

Önce Moleküler Mekanik Metodu spiro-[5,4]-1-halo-6,9-dioksodekan ve spiro-[5,5]-1-halo-6,10-dioksoundekan (2) ye uygulanmıştır (halojen = klor veya brom). Teorik sonuçlar halojenin, (2) sisteminde dikey, (1) sisteminde yatay konumu tercih ettiğini gösterip Zefirov ve grubunun deneysel sonuçlarına uymaktadır.

Sonra Moleküler Mekanik Metodu spiro-[5,4]-1-nitro-6,9-dioksodekan ve spiro-[5,5]-1-nitro-6,10-undekan'a uygulanmış ve teorik sonuçlar nitro grubunun her iki sistemde de (1) ve (2) yatay konumu tercih ettiğini göstermiştir.

Son olarak nitro (1), nitro (2) ve bunların 4-t-bütil

türevlerinin sentezleri gerçekleştirilip halka çevrilmesi ile dengede bulunan konformerlerin arasındaki serbest enerji farkı Nükleer Manyetik Resonans (NMR) ile bulunmuştur. Deneysel sonuçlar, teorik hesaplara uyum göstermiştir.

Nitro grubu daha önceleri de yapısı, boyutları elektronik dağılımı ve yük taşıması itibarı ile halojenlerden farklı tavır göstermiştir. Bu çalışmada Nitro grubunun özelliği bir kere daha hem deneysel hem teorik açıdan kanıtlanmıştır.

TABLE OF CONTENTS

LIST OF FIGURES

LIST OF TABLES

LIST OF SYMBOLS

E	energy
E_b	bond stretching energy
E_θ	bond angle bending energy
E_w	bond torsion energy
E_{vdw}	Van der Waals interactions energy
E_{es}	electrostatic energy
LP	lone pair
ε	hardness parameter
r^*	Van der Waals radius
r	distance
w	dihedral angle
δ_q	ratio of bond dipole to bond length
δ	chemical shift (NMR)
ΔG	conformational free energy difference
LR	long range
R	1.987 cal/mole
T	temperature (^oK)
K	equilibrium constant

CHAPTER I

1.1. Introduction

It is well known that all the theoretical results in chemistry should be in accordance with the solutions of the Schroedinger equation. However, a number of other theoretical approximations are shown to be just as applicable[1]. Among these methods, Molecular Mechanics calculations give satisfactory results especially in quantifying the energy of a given molecular conformation[2]. This has led chemists to study various interactions in detail. Parameters have been derived by comparison of calculated and observed molecular properties. Functions which relate energy to geometrical parameters of the molecular conformations have been derived indirectly from various empirical sources as spectroscopic and thermodynamic data[3]. Several good Molecular Mechanics methods have emerged from the calculations on large sets of molecules on a trial and error basis[4]. The various names under which this topic has been known reflect its history: Westheimer Method, Strain Energy Minimization Technique, Force Field Calculations, and Molecular Mechanics which is the accepted modern term.

A molecular Force Field describes the potential energy

CHAPTER I

1.1. Introduction

It is well known that all the theoretical results in chemistry should be in accordance with the solutions of the Schroedinger equation. However, a number of other theoretical approximations are shown to be just as applicable[1]. Among these methods, Molecular Mechanics calculations give satisfactory results especially in quantifying the energy of a given molecular conformation[2]. This has led chemists to study various interactions in detail. Parameters have been derived by comparison of calculated and observed molecular properties. Functions which relate energy to geometrical parameters of the molecular conformations have been derived indirectly from various empirical sources as spectroscopic and thermodynamic data[3]. Several good Molecular Mechanics methods have emerged from the calculations on large sets of molecules on a trial and error basis[4]. The various names under which this topic has been known reflect its history: Westheimer Method, Strain Energy Minimization Technique, Force Field Calculations, and Molecular Mechanics which is the accepted modern term.

A molecular Force Field describes the potential energy

of a molecule relative to the energy of a reference geometry (strain-free, or natural geometry). The Molecular Mechanics Method can predict conformational energies, geometries of most stable conformations, intimate transition state geometries and energies in organic reactions.

Many acyclic and alicyclic alkanes have been studied sytematically and detailed theoretical information is available on their structures, conformational energies and the barriers to internal rotation[5]. Studies of functional derivatives of alkanes have been fewer and less systematic[6]. While calculations have been highly succesful for hydrocarbons and some classes of compounds, such as silanes, carbonyl compounds and alkenes, only little work has been reported about the development of force fields capable of handling molecules containing ether oxygen[7].

Allinger and Chung have calculated energies and structures of some oxa compounds[8].

Ulrich Burkert has studied geometries and energies of polymethyl-1,3-dioxanes[9] and simple alcohols[10].

Allinger et al.[11] have studied oxane and 1,3-dioxane rings and examined a number of interesting conformational problems.

Meyer, Allinger and Yuh[12] have reported on mono- and non-geminal dihaloalkenes and monohaloketones.

The potential energy of a molecular conformation may be expressed as a function of several parameters[13].

$$E_{total} = E_b + E_\theta + E_w + E_{vdw} + E_{es} \qquad \text{Eq.1.1.1}$$

These parameters depend on internal coordinates and interatomic distances.

In Eq.1.1.1 the first term E_b (bond stretching) is significant if there are in the molecule one or more bonds which are forced to have unnatural bond lengths. It is generally agreed that it costs much less energy to bend a bond than to stretch or to compress it[14,15], and consequently this term is usually negligible in comparison to other terms in Eq.1.1.1.

The second term E_θ (bond angle bending) associates energy with bending a single bond from the regular tetrahedral (109.47°). If an atom has a symmetrical tetrahedral arrangement it will have bond angles of 109.47°. If the atom has different groups attached to it, the angles are not exactly tetrahedral. The differences may result from bonding (hybridization), Van der Waals repulsions, hydrogen bonding etc... The simplest approach is to say that $\pm 3^\circ$ deviation from tetrahedral[16] corresponds to zero bond angle bending energy, and if deviation is more than ±3 degrees, than needs to be considered[16]. E_θ is proportional to the square of the bending. Distorting two angles costs only half as much as distorting one angle and hence strain tends to distribute itself through out a system, rather than being concentrated in one place.

The third term E_w (bond torsion) relates rotational barrier to the variation in dihedral angle, w. However, the origins of the torsional interactions are not well understood[17].

The fourth term E_{vdw} (Van der Waals) represents the non-bonded interactions in terms of the Van der Waals function[18] (discussed in detail in 3.2).

The fifth term E_{es} (electrostatic) arises when there are two or more polar groups in the molecule. The charge-dipole interactions in molecules which contain both a charge and a dipole should also be considered. E_{es} term can than be expressed as in Eq.1.1.2.

$$E_{es} = E_{dipole\text{-}dipole} + E_{charge\text{-}dipole} \qquad \text{Eq.1.1.2}$$

Calculation of induced dipole interactions may be required for very detailed studies. The order of magnitude of dipole-induced dipole interactions are generally small compared to the order of magnitude of dipole-dipole and charge-dipole interactions therefore they have been neglected in this work[19]. Electrostatic interactions are discussed in detail in 3.3.

Along with these five parameters the matrix effects such as dielectric constant of the medium and concentration are important and should be taken into consideration[20].

In this study first a theoretical approach is

attempted to determine the conformational free energy difference between the conformers I and II of spiro[5,4]-1-halo-6,9-dioxodecane (1), and spiro-[5,5]-1-halo-6,10-dioxoundecane (2) in figure 1.1.1 with the Molecular Mechanics method. In figure 1.1.1, X is chlorine or bromine. The results of the calculations are than compared to the experimental results reported in the literature[21], and are found to be in good agreement. Finally, the set of parameters derived are than used to carry out calculations for the conformers of 2-nitro-cyclohexanone ethylene and propylene glycol ketals and are compared to the experimental results of this work, determined by using Nuclear Magnetic Resonance parameters.

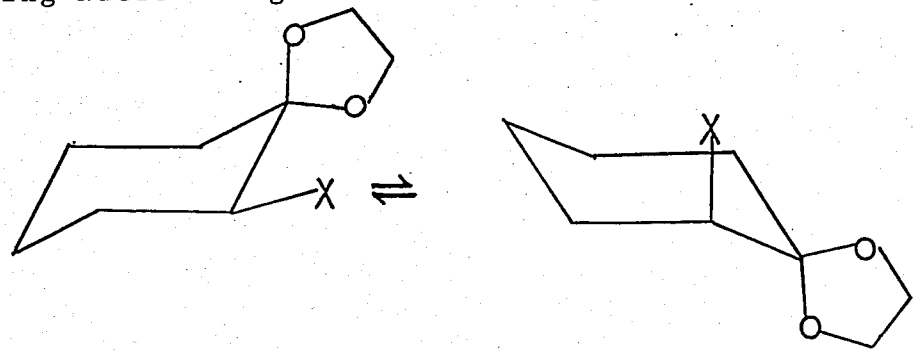

I ⇌ II

1

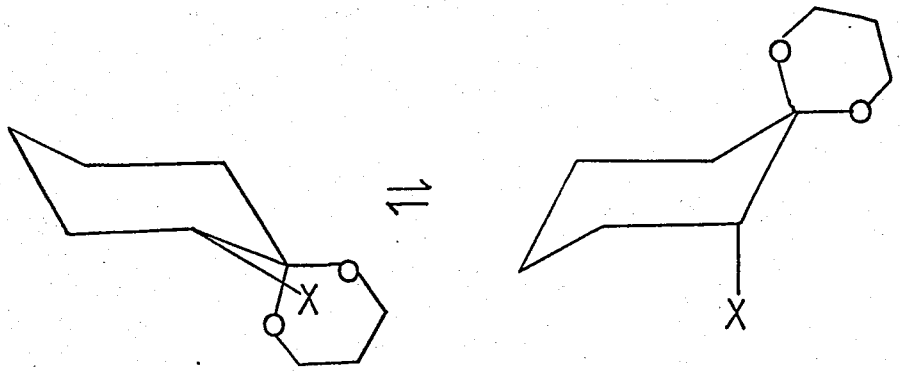

I ⇌ II

2

Figure 1.1.1. Conformers of (1) and (2)

CHAPTER 2

2.1. Description of Model Compounds

Molecular Mechanics has been easily applied to simple hydrocarbons and used widely in the literature[22]. Methods have been extended to compounds containing heteroatoms but little work has been reported on compounds containing ether oxygen[23].

The compounds under investigation contain ether oxygen. Complications occur due to the presence of the oxygen lone pair electrons.

U.Burkert[24] has treated lone pairs of 1,3-dioxanes and alcohols as point charges taken from quantum mechanical calculations with weak Van der Waals interactions between lone pairs. In an alternative treatment Allinger and Chang[25] have included lone pair electrons as a pair of additional pseudoatoms. They report that the electron pair is assigned Van der Waals characteristics like an atom. The size (Van der Waals radius), hardness (ε), and position is chosen so as to fit experimental data. Using the conformational free energy of the methyl group is 5-methyl-1,3-dioxane and the conformational free energy of the t-butyl group in 5-t-bu-1,3-dioxane they have fitted the two parameters, ε, and the r*

Van der Waals radius. The position of the lone pair was established by integrating along an sp^3 hybrid (assuming lone pairs occupy an orbital which is approximately sp^3) with the appropriate nuclear charge and locating the center of electron density. The results are shown in Table 2.1.1. Later Allinger et. al.[26] have changed the Van der Waals characteristics of the oxygen atom. They have put less emphasis on the lone pairs and more on the core, Table 2.1.1. Once the problems created by the presence of ether oxygen are solved by adopting the description for oxygen and lone pairs in the literature, one has to establish the geometries of the conformers under investigation.

Table 2.1.1. Properties of Oxygen and Lone Pairs

Reference	Atom	(kcal/mole)	bond moment (D)	r*(Å)
25	0	0.002	0.73	1.65
25	LP	0.025	0.60	1.20
26	0	0.050	0.40	1.79
26	LP		0.90	

2.2. Conformers of (2)

Cyclohexanone propylene glycol ketal, (2) has two six-membered rings. It is expected that cyclohexane and most of its derivatives are in the chair form since the chair form is free of angle strain, torsional strain and Van der Waals strain[27]. The chair form and the flexible forms of cyclo-

hexane were recognized by Sachse (1892)[28]. He also realized that there could be two monosubstitution products of the rigid or chair form (one that we call now axial substituent and the other equatorial substitutent) which could be interconverted by a process of chair inversion and would thus be in dynamic equilibrium, figure 2.2.1. (2), having two six-membered rings may exist in four different "chair-chair conformers" as in figure 2.2.2.

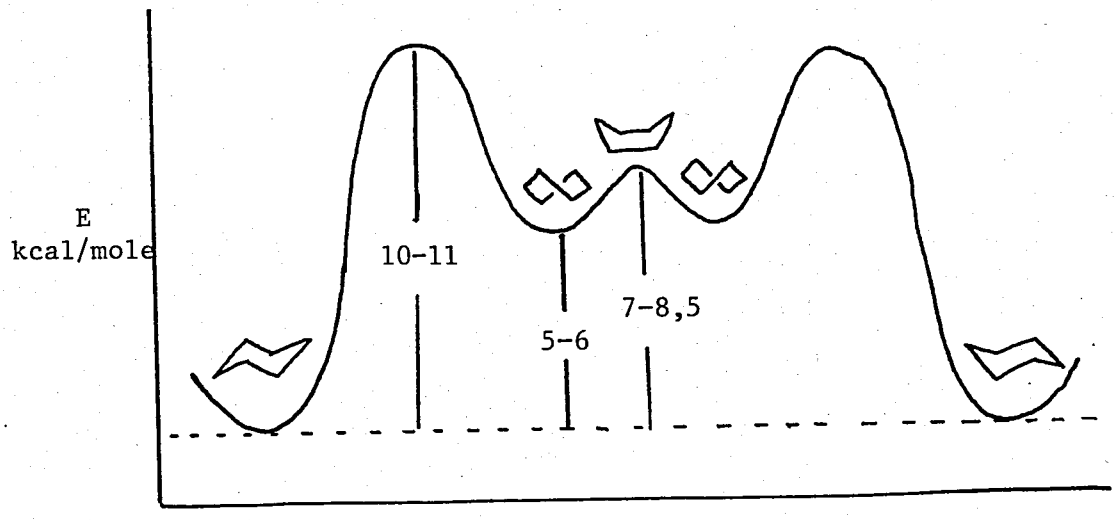

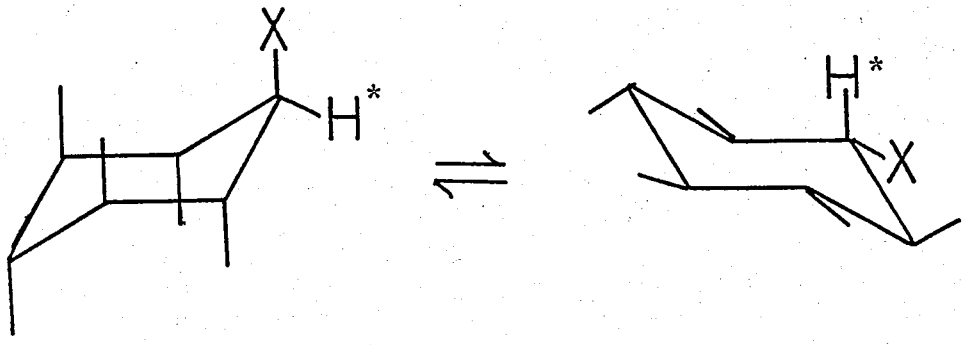

chair-chair inversion

(*α-proton)

Figure 2.2.1. Chair inversion and energy profile

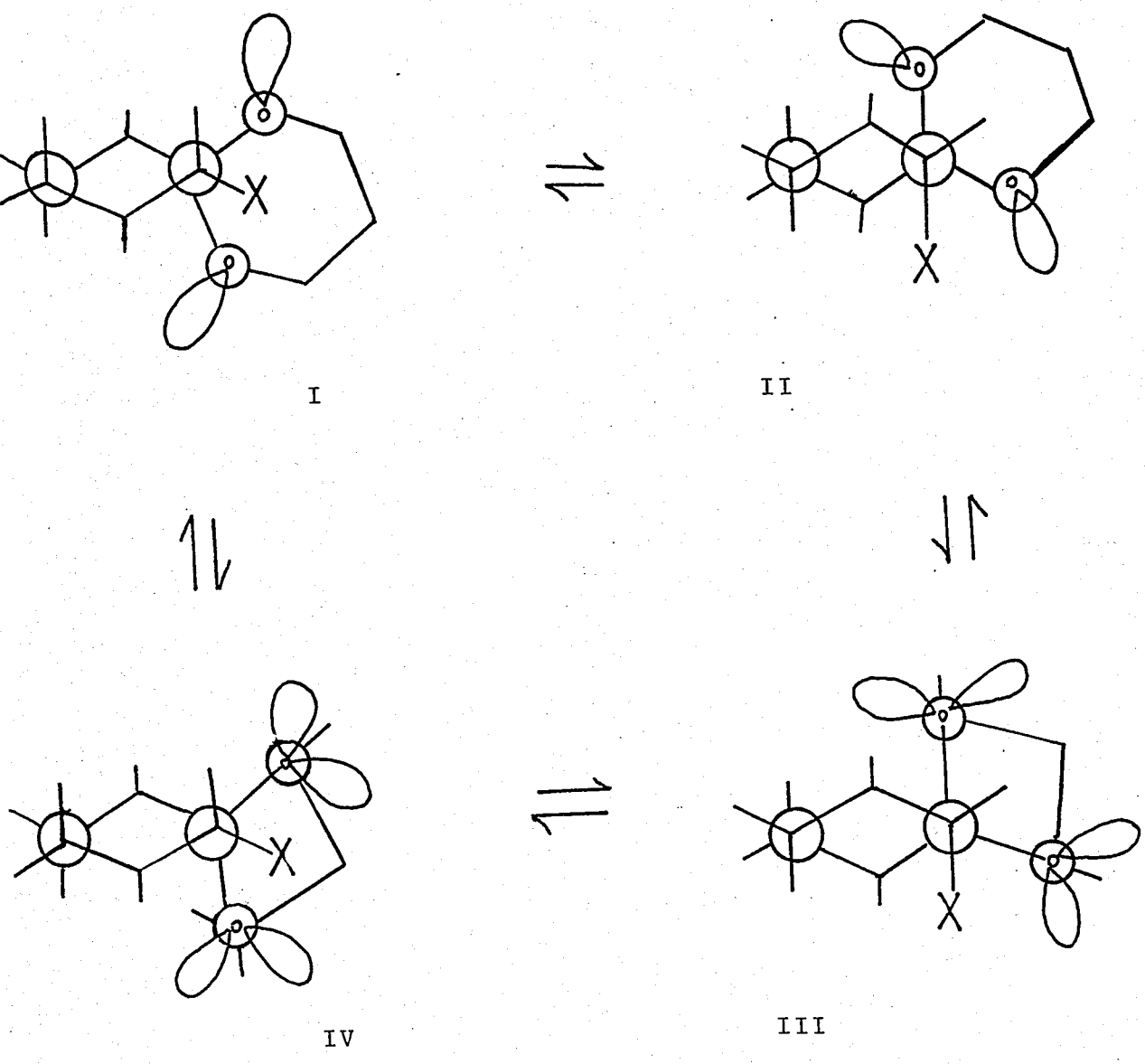

Figure 2.2.2. Conformation of propylene glycol ketals of 2-halocyclohexanones (2)

In figure 2.2.2. cnoformers I and II have lone pairs away from X, where as conformers III and IV have lone pairs facing toward X. The conformers are drawn in such a way that one can observe the position of X in relation to the lone pairs and the interconverting ring systems.

2.3. Conformers of (1)

To establish the conformation of cyclohexanone ethylene glycol ketal, (1), one has to choose among the planar, envelope and the half-chair conformations of the five-membered ring, Table 2.3.1.

Table 2.3.1. Conformers of Cyclopentane and Torsional Angles(29)

	planar	envelope	half chair
$w_{12}=w_{51}$	0^o	46.1^o	15.15^o
$w_{23}=w_{45}$	0^o	28.6^o	39.45^o
w_{34}	0^o	0^o	48.1^o

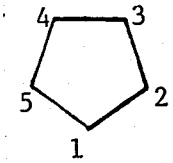

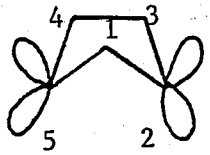

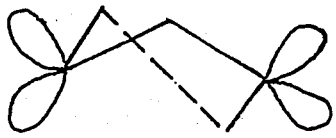

Torsional angles are described in Figure 2.3.1.

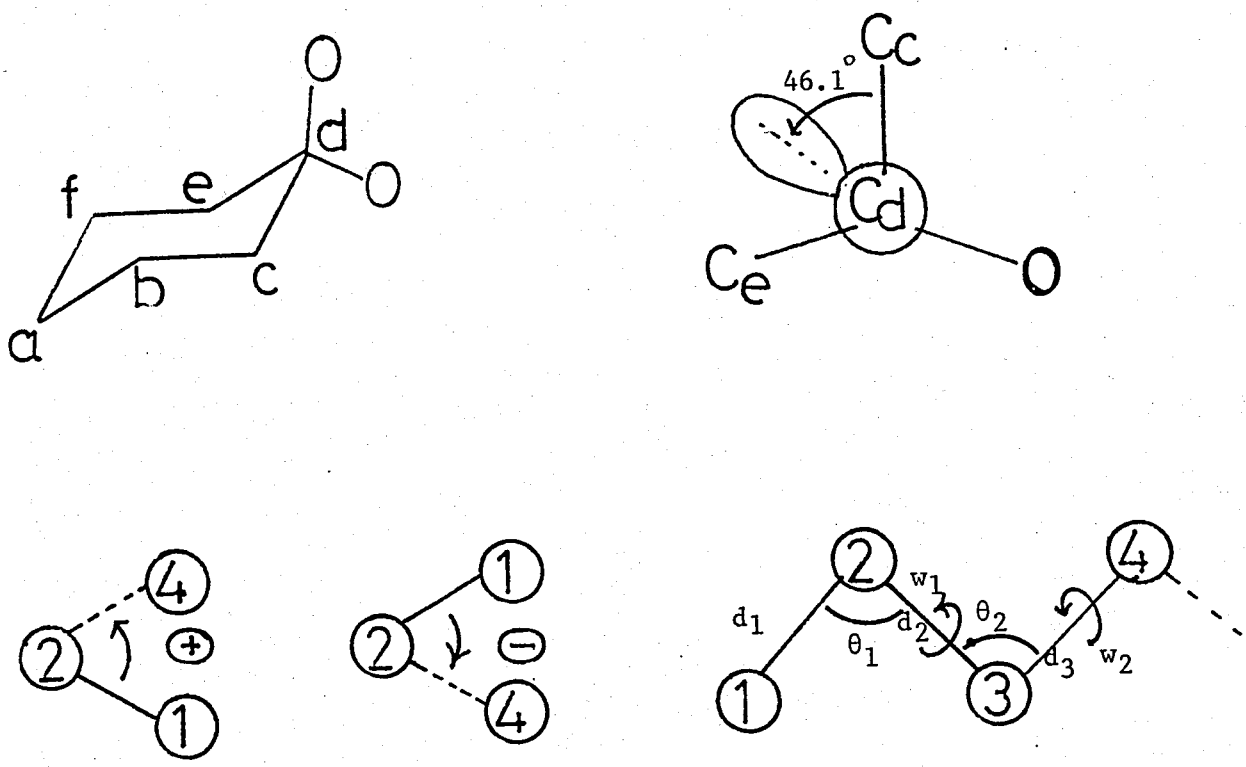

Figure 2.3.1. Torsional (dihedral) angles

Large dihedral angles (w_{12}=w_{51}) enable the X substituent to be further away from the lone pairs in the envelope conformation compared to that of the planar and half-chair conformations. The two chair forms of the six-membered ring and the two envelope forms of the five-membered ketal ring add up to four possible conformers, as in figure 2.3.2.

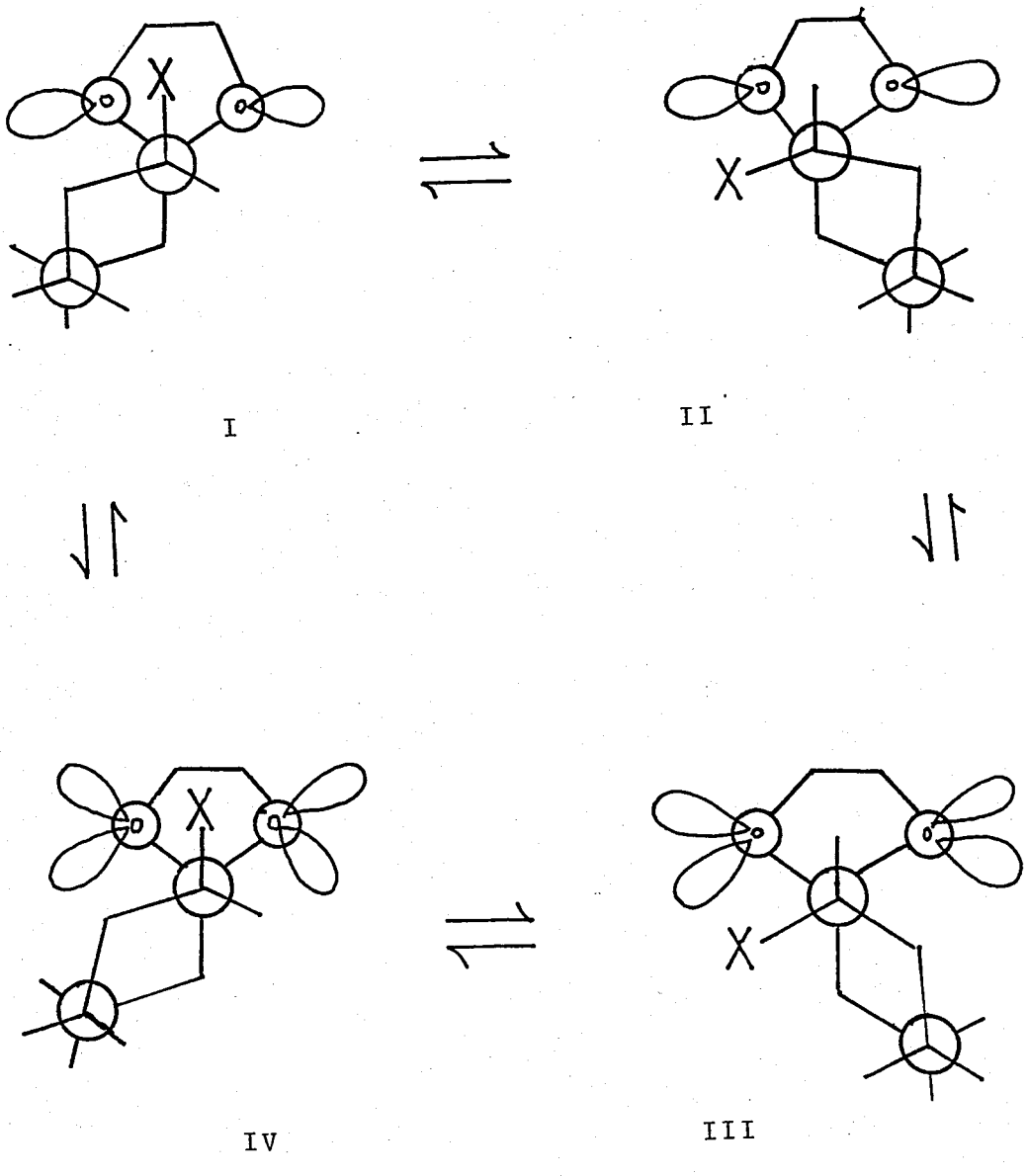

Figure 2.3.2. Conformation of ethylene glycol ketals of 2-halacyclohexanones (1)

CHAPTER 3

3.1. Interactions

In determination of conformational free energy by molecular mechanics, the interaction of each atom with every other atom in the molecule should be considered. As the conformation of the molecule changes, the interactions between a given pair of atoms may change or may stay the same. The interactions which are equivalent in the equilibrating conformers need not be calculated since their difference will be eliminated in conformational free energy calculations. The most critical interactions that may exist between atom pairs in the conformers of (1) and (2) are shown in figure 3.1.1. and are listed in table 3.1.1.

The important interactions which are effective in altering the sign and magnitude of the conformational free energy difference are:

1) 1,1-oxygens and the 2-substituent (i.e. # 2 in table 3.1.1).

2) Lone pairs in oxygen atoms and the 2-substituent (i.e. #1 in table 3.1.1).

3) 1,3-Syn-axial and long range interactions (i.e. # 3 in table 3.1.1).

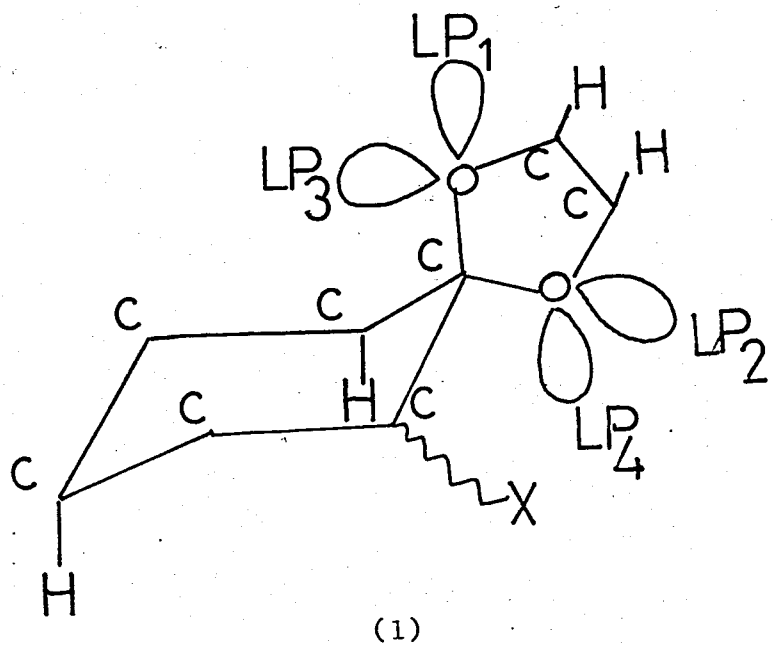

(1)

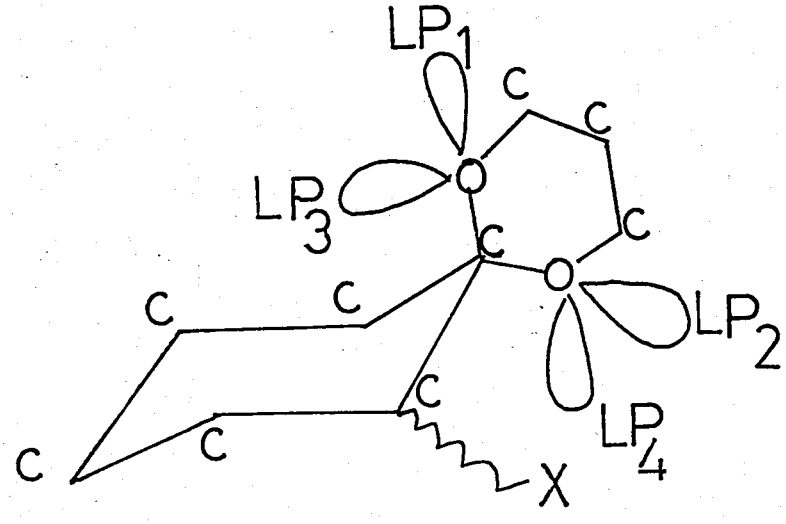

(2)

Figure 3.1.1

Table 3.1.1. Types of Interactions and Examples

	Interaction	Examples
1.	LP-X	LP_1-X, LP_4-X
2.	X-O	X-O_1, X-O_2
3.	X-H	X-H_4, X-H_7^*
4.	O-H	O_1-H_8, O_2-H_6
5.	LP-H	LP_1-H_6, LP_2-H_7
6.	X-C	X-C_8, X-C_3
7.	O-C	O_1-C_8, O_1-C_6
8.	LP-C	LP_1-C_8, LP_3-C_5
9.	C-C	C_2-C_5, C_5-C_7
10.	H-H	H_4, -H_6, H_6, -H_8
11.	LP-O	LP_2-O_1-LP_3-O_2

*These types of interactions will be referred to as Long Range Interaction (LR) from here on.

The dihedral angles that are required for the calculations of the interactions listed above are X-C-C-O and C-C-O-LP. These angle are shown in Figure 3.1.2. and Tables 3.1.2. and 3.1.3.

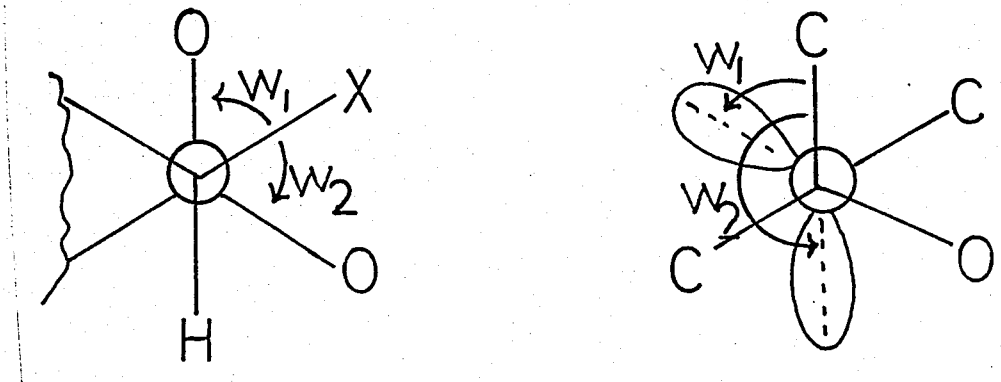

Figure 3.1.2. Dihedral angles

Table 3.1.2. Ethylene Glycol Ketal (1) dihedral angles X-C C-O(w_1) and C-C-O-LP (w_2)[30]

	w_1	w_2		w_1	w_2
I*	60	46.1	III	-60	-46.1
	-60	-46.1		180	46.1
	60	166.1		-60	73.9
	-60	-166.1		180	-73.9
II	-60	46.1	IV	60	-46.1
	180	-46.1		-60	46.1
	-60	166.1		60	73.9
	180	-166.1		-60	-73.9

*I, II, III, IV refer to conformers in Figures 2.2.2 and 2.3.2.

In Table 3.1.2. the five-membered ring is taken to be the envelope form with the angle given in Table 2.3.1. The other angles are measured from Dreiding models upon construction of (1).

The sign and magnitude of the important interactions may vary with interatomic distances. The interatomic distances for the oxygen-2-substituent interactions were calculated by making use of coordinates of atoms in cyclohexane assigned by Eliel and Allinger[31] as shown in Figure 3.1.3. Bond lengths[32] used are shown in Table 3.1.4.

Table 3.1.3. Propylene Glycol Ketal (2) dihedral angles X-C-C-O (w_1) and C-C-O-LP (w_2)[30]

	w_1	w_2		w_1	w_2
I	60	60	III	180	-60
	-60	-60		60	60
	60	180		180	60
	-60	180		60	-60
II	180	60	IV	60	-60
	60	-60		-60	60
	180	180		60	60
	60	180		-60	-60

Table 3.1.4. Bond lengths[32]

Bond	length (Å)
C-C	1.54
C-O	1.43
O-LP	0.6
C-Cl	1.76
C-Br	1.91
C-H	1.09

The distances were calculated with the classical formula Eq.3.1.1.

$$r = \left[(x_2-x_1)^2 + (y_2-y_1)^2 + (z_2-z_1)^2\right]^{1/2} \qquad \text{Eq.3.1.1}$$

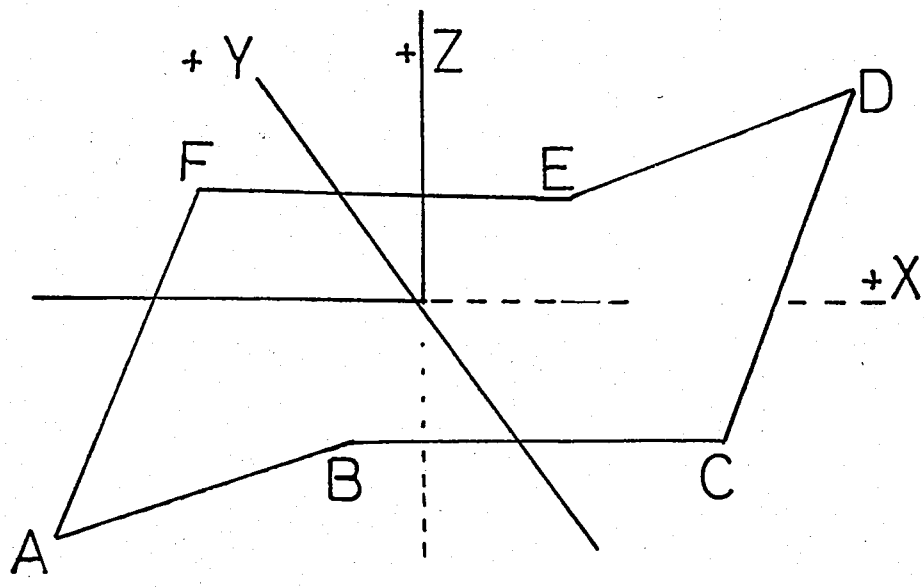

Figure 3.1.3. Cartesian Coordinates of Cyclohexane[31]

SUBSTITUENT COORDINATES

		X	Y	Z
A	ax	-1.325+0.223d	0	-0.651-0.975d
	eq	-1.325-0.997d	0	-0.651+0.077d
B	ax	-0.764-0.333d	-1.263-0.067d	0.940d
	eq	-0.764-0.333d	-1.263-0.804d	-0.492d
C	ax	0.764+0.333d	-1.263-0.067d	-0.940d
	eq	0.764+0.333d	-1.263-0.804d	0.492d
D	ax	1.325-0.223d	0	0.651+0.975d
	eq	1.325-0.997d	0	0.651-0.077d
E	ax	0.764+0.333d	1.263+0.067d	-0.940d
	eq	0.764+0.333d	1.263+0.804d	0.492d
F	ax	-0.764-0.333d	1.263+0.067d	0.940d
	eq	-0.764-0.333d	1.263+0.804d	-0.492d

Figure 3.1.3. cont.

H-SUBSTITUENT COORDINATES

		X	Y	Z
A	ax	-1.079	0	-1.727
	eq	-2.426	0	-0.565
B	ax	-1.132	-1.337	+1.038
	eq	-1.132	-2.151	-0.543
C	ax	1.132	-1.337	-1.038
	eq	1.132	-2.151	0.543
D	ax	1.079	0	1.727
	eq	2.426	0	0.565
E	ax	1.132	1.337	-1.038
	eq	1.132	2.151	0.543
F	ax	-1.132	1.337	1.038
	eq	-1.132	2.151	-0.543

where r is the distance between the atoms, and x, y and z are the coordinates of the interacting atoms. The lone pair-2-substituent distances were calculated with equations[33] 3.1.2, 3.1.3, and 3.1.4 shown below.

$$X_2-X_1=(d_3-d_4\cos\theta_3)\cos\theta_2+d_4\sin\theta_2\sin\theta_3\cos w_2-(d_2-d_1\cos\theta_1) \quad \text{Eq.3.1.2}$$

$$Y_2-Y_1=(d_3-d_4\cos\theta_3)\sin\theta_2-d_4\cos\theta_2\sin\theta_3\cos\theta_2-d_1\sin\theta_1\cos w_1 \quad \text{Eq.3.1.3}$$

$$Z_2-Z_1=-d_4\sin\theta_3\sin\theta_2-d_1\sin\theta_1\sin w_1 \quad \text{Eq.3.1.4}$$

The formulas 3.1.2, 3.1.3, and 3.1.4 take the forms shown below when bond lengths shown in Table 3.1.4. and tetrahedral bond angles are substituted in place of d_i and θ_i in the formulas.

For chlorine-lone pair interaction:

$$X_2-X_1 = -2.6717 + 0.5331 \cos w_2 \qquad \text{Eq.3.1.5}$$

$$Y_2-Y_1 = 1.5368 + 0.1888 \cos w_2 - 1.659 \cos w_1 \qquad \text{Eq.3.1.6}$$

$$Z_2-Z_1 = -0.5656 \sin w_2 - 1.659 \sin w_1 \qquad \text{Eq.3.1.7}$$

For bromine-lone pair interactions:

$$X_2-X_1 = -2.7218 + 0.5331 \cos w_2 \qquad \text{Eq.3.1.8}$$

$$Y_2-Y_1 = 1.5368 + 0.1888 \cos w_2 - 1.8004 \cos w_1 \qquad \text{Eq.3.1.9}$$

$$Z_2-Z_1 = -0.5656 \sin w_2 - 1.8004 \sin w_1 \qquad \text{Eq.3.1.10}$$

For hydrogen-lone pair interactions:

$$X_2-X_1 = -2.4494 + 0.5331 \cos w_2 \qquad \text{Eq.3.1.11}$$

$$Y_2-Y_1 = 1.5368 + 0.1888 \cos w_2 - 1.0312 \cos w_1 \qquad \text{Eq.3.1.12}$$

$$Z_2-Z_1 = -0.5656 \sin w_2 - 1.0312 \sin w_1 \qquad \text{Eq.3.1.13}$$

When w_1 and w_2 from tables 3.1.2. and 3.1.3. are substituted for different conformers of (1) and (2), the resulting X_2-X_1, Y_2-Y_1 and Z_2-Z_1 values can be inserted in the classical distance formula Eq.3.1.1. The distances obtained for the different conformers of (1) and (2) are tabulated in Table 3.1.5 and 3.1.6. These distances can be seen in Figure 3.1.4.

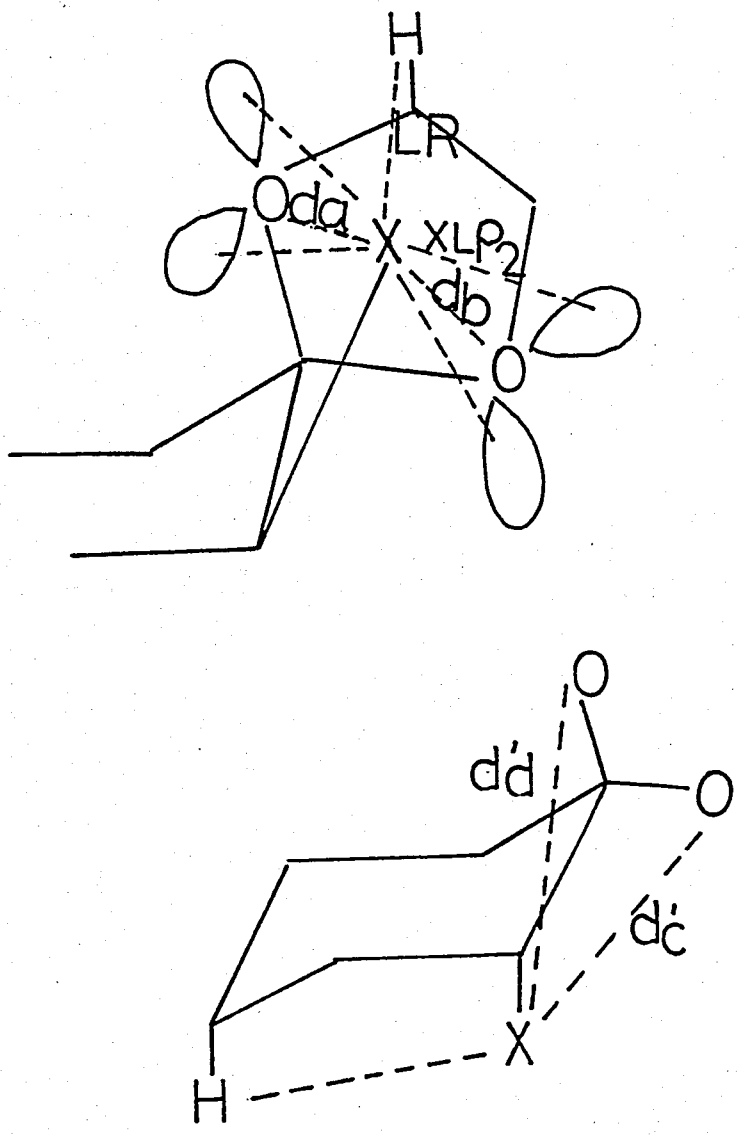

Figure 3.1.4. Intramolecular distances

Table 3.1.5. Intramolecular distances (Å) for (1)

		X = Cl	X = Br	X = H
	da=db	2.95	3.04	2.63
	dc'	2.95	3.04	2.63
	dd'	3.96	4.11	3.36
I	$X-LP_1$	3.066	3.161	2.710
	$X-LP_2$	3.066	3.161	2.710
	$X-LP_3$	3.594	3.684	3.250
	$X-LP_4$	3.594	3.684	3.250
	LR	3.514	3.574	
II	$X-LP_1$	2.657	2.729	2.426
	$X-LP_2$	4.066	4.210	3.431
	$X-LP_3$	3.484	3.567	3.174
	$X-LP_4$	4.389	4.523	3.809
	1,3 syn-Ax	2.795	2.843	
III	$X-LP_1$	3.066		
	$X-LP_2$	4.066		
	$X-LP_3$	2.790		
	$X-LP_4$	4.149		
	1,3 syn-Ax	2.795		
IV	$X-LP_1$	2.657		
	$X-LP_2$	2.657		
	$X-LP_3$	3.297		
	$X-LP_4$	3.297		
	LR	4.2		

Table 3.1.6. Intramolecular Distances (Å) for (2)

		X = Cl	X = Br	X = H
	da=db	2.95	3.04	2.63
	dc'	2.95	3.04	2.63
	dd'	3.96	4.11	3.36
I	$X-LP_1$	3.184	3.280	2.815
	$X-LP_2$	3.184	3.280	2.815
	$X-LP_3$	3.550	3.684	3.223
	$X-LP_4$	3.550	3.684	3.223
	LR	1.996	2.031	
II	$X-LP_1$	4.105	4.229	3.478
	$X-LP_2$	2.706	2.776	2.484
	$X-LP_3$	4.395	4.528	2.999
	$X-LP_4$	3.550	3.684	3.223
	1,3 Syn-Ax	2.795	2.843	
III	$X-LP_1$	4.105		
	$X-LP_2$	3.184		
	$X-LP_3$	4.105		
	$X-LP_4$	2.706		
	1,3 Syn-Ax	2.795		
IV	$X-LP_1$	2.706		
	$X-LP_2$	2.706		
	$X-LP_3$	3.184		
	$X-LP_4$	3.184		
	LR	4.6		

Conformer IV in Figure 2.2.2. resembles 5-hetero-substituted-1,3-dioxane, Figure 3.1.5.

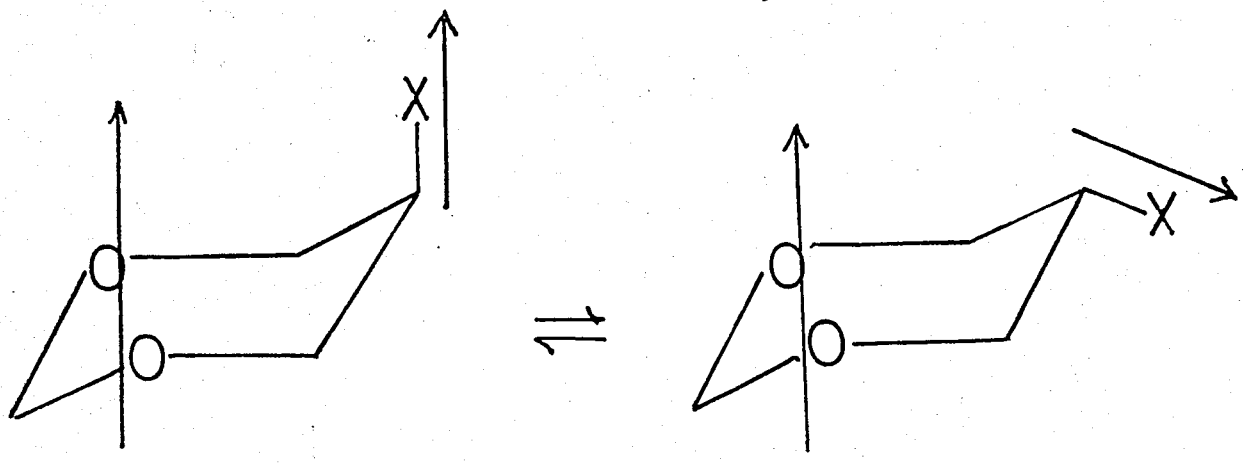

Figure 3.1.5. 5-heterosubstituted-1,3-dioxane

As shown in figure 3.1.5. the ring dipole and the substitutent dipole are involved in parallel allignment of the dipoles in (A), whereas a nearly antiparallel arrangement of the two dipoles is observed in (B); implying that B is less repulsive electrostatically thus a more probable conformer.

Eliel and Coworkers[34], in their systematic study of 5-heterosubstituted-2-isopropyl-1,3-dioxanes, have reported chlorine and bromine to prefer equatorial conformations (Cl: 1.20, Br: 1.44 kcal/mole). Juaristi[35] reports that in contrast to O/F and O/CN attractive gauche interactions, O/I, O/Br and O/Cl gauche interactions are repulsive in 1,4-heterobutane segments and that these are "special effects" which can not be explained in terms of Eq.1.1.1.

Cursory inspection of Tables 3.1.5. and 3.1.6 show that both (1) and (2) exist most probably in equilibrium I<=>II in figure 2.2.2 and figure 2.3.2. since they represent atoms farther apart. Namely the oxygens and the 2-substituent, also the lone-pairs and the 2-substituent are removed from each other by longer distances in I<=>II. Based on the information given above I and II of (1) and (2) were chosen to be model compounds on which molecular mechanics were to be applied.

Rewriting equation 1.1.1. in the form of the conformational free energy difference it becomes Eq.3.1.14.

$$\Delta E=\Delta E_b+\Delta E_\theta+\Delta E_w+\Delta E_{vdw}+\Delta E_{es} \qquad \text{Eq.3.1.14}$$

Since the structures taken do not have unnaturally strained bonds, and angles, it is reasonable to assume that same kind of bonds have invarient bond lengths in equilibrating conformers also that the angles are tetrahedral in both conformormers I<=>II. This assumption results in $\Delta E_b=0$ and $\Delta E_\theta=0$ and the first two terms ΔE_b and ΔE disappear in Eq. 3.1.14.

The sum of torsional strains about individual bonds is usually close to zero for simple cyclohexane rings[36] and almost perfectly staggered geometry exist. It is assumed that (2) is almost perfectly staggered and that $\Delta E_w=0$ for the equilibrating conformers (2). For (1) system, a

torsional strain small in magnitude may exist. The torsional strains are shown to be small[37] and it is assumed that ΔE_w will not be very significant. Therefore only ΔE_{vdw} and ΔE_{es} are considered in this study.

3.2. Steric Interactions

Steric Interactions are represented by Van der Waals function. In theory this function is composed of two parts. At longer distances (r), the forces between the two atoms are attractive. At shorter distances, atoms come sufficiently close that their Van der Waals radii interpenetrate and intense repulsive forces develope. The sum of the repulsions between nucleii and between electrons outweighs attractive force. The combination of these forces lead to the Van der Waals function. Hill[38] has formulated these forces in Eq.3.2.1.

$$E_{vdw} = -2.25\varepsilon\alpha^{-6} + 8.28\ 10^5\ \varepsilon \exp\frac{-\alpha}{0.0736} \qquad \text{Eq.3.2.1}$$

In Eq.3.2.1. α is a function of distance and is represented by Eq.3.2.2. where r is the distance between the atoms and r* is the Van der Waals radius.

$$\alpha = \frac{r}{r^*_x + r^*_y} \qquad \text{Eq.3.2.2}$$

Eq.3.2.2. determines Eq.3.2.1. to be attractive or repulsive when α is close to 1 Eq.3.2.1. is attractive, when α is

less than 0.8937 Eq.3.2.1. is repulsive. In Eq.3.2.1. ε is a function of energy. It is a measure of magnitude of interacting forces and varies with the size of the atom. ε is called the hardness parameter showing the hardness of the electron-cloud around the atom. ε is represented in Eq.3.2.3

$$\varepsilon = \sqrt{\varepsilon_x \varepsilon_y} \qquad \text{Eq. 3.2.3}$$

The Van der Waals parameters used are in Table 3.2.1.

Table 3.2.1. Van der Waals Parameters

Ref.	X	r_x^* (Å)	ε_x kcal/moles
27	Cl	1.95	0.214
27	Br	2.10	0.296
28	O	1.65	0.002
28	LP	1.20	0.025
27	H	1.50	0.063

The properties of the lone pair are such that the properties of the rest of the oxygen are modified as well. Modifications retain a total assembly (oxygen + lone pair) which show reasonable characteristics when approached by other closed shell species[28].

Values of the Van der Waals Interactions calculated according to Eq.3.2.1 with parameters of Table 3.2.1 are shown in Table 3.2.2. and 3.2.3. In these tables the negative

values show attractive interactions and the positive values show repulsive interactions. It can be observed that in both tables the lone pair-2-substituent and oxygen-2-substituent interactions are generally small in magnitude. The long range interactions in (1) system are also attractive and small in magnitude. In (2) system, however, esentially in conformer I severe long range interactions take place. The magnitude of these interactions are such that conformer I should not exist at all. These interactions can be seen clearly in figure 2.2.2. where the X-substituent is unfavorably extended over the dioxane ring system.

Table 3.2.2. Van der Waals Interactions (kcal/moles) Ethylene Glycol Ketals (1)

		X=Cl	X=Br
I	da=db	0.098	0.137
II	dc'	0.098	0.137
	dd'	-0.021	-0.024
I	X-LP_1	-0.084	-0.092
	X-LP_2	-0.084	-0.092
	X-LP_3	-0.063	-0.082
	X-LP_4	0.063	0.082
II	X-LP_1	-0.181	-0.336
	X-LP_2	-0.034	-0.048
	X-LP_3	-0.072	-0.091
	X-LP_4	-0.022	-0.029
I	LR	-0.122	-0.156
II	1,3 Syn-Ax	0.669	1.78
I	E_{vdw} total	-0.342	-0.386
II	E_{vdw} total	1.468	3.840

Table 3.2.3. Van der Waals Interactions (kcal/moles) Propylene Glycol Ketals (2)

		X=Cl	X=Br
I	da=db	0.098	0.137
II	dc'	0.098	0.137
	dd'	-0.021	-0.024
I	L-LP_1	-0.088	-0.095
	X-LP_2	-0.088	-0.095
	X-LP_3	-0.066	-0.082
	X-LP_4	-0.066	-0.082
II	X-LP_1	-0.033	-0.042
	X-LP_2	0.173	0.288
	X-LP_3	-0.022	-0.028
	X-LP_4	-0.066	-0.082
I	LR	>30	>50
II	1,3 Syn-Ax	0.669	1.78
I	E_{vdw} total	>30	>50
II	E_{vdw} total	1.467	3.809

Summation of the Van der Waals Interactions in table 3.2.2. show that conformer I of (1) system has attractive interactions whereas conformer II has repulsive interactions. Therefore (1) prefers conformation I upon consideration of Table 3.2.2. Summation of the Van der Waals Interactions in Table 3.2.3. show that conformer II of (2) system is more stable than conformer I. In fact the magnitudes of conformer

I show the non-existance of this conformer.

3.3. Electrostatic Interactions

Electrostatic Interactions between two dipoles have generally been calculated by the Jeans equation Eq.3.3.1[39].

$$E_{\mu} = \frac{\mu_1 \mu_2}{Dr^3}(\cos\chi - 3\cos\alpha_1 \cos\alpha_2) \qquad \text{Eq.3.3.1}$$

$$\cos\chi = \sin\theta_1 \sin\theta_2 \cos w - \cos\theta_1 \cos\theta_2 \qquad \text{Eq.3.3.2}$$

$$\cos\alpha_1 = a^2 + R^2 - c^2 - b^2 + 2bc\cos\theta_2 \qquad \text{Eq.3.3.3}$$

$$\cos\alpha_2 = b^2 + R^2 - a^2 - c^2 - 2ac\cos\theta_1 \qquad \text{Eq.3.3.4}$$

The derivation of this equation assumes the two interacting dipoles to be far apart compared with their effective lengths. If the separation and length of dipoles are similar, this approximation could be leading to errors. An alternative method to calculate electrostatic interaction energy has been used in the literature, where each dipole is treated as two point charges[40]. The coulombic interactions between pairs of point charges are calculated according to equation 3.3.5.

$$Eq = \frac{1}{D} \Sigma \frac{\delta q_i \, \delta q_j}{r_{ij}} \qquad \text{Eq.3.3.5}$$

In equation 3.3.5, D is the dielectric constant and δq_i and δq_j are the ratio of bond dipole to bond length as calculated in Eq.3.3.6.

$$\delta q = \frac{\text{bond dipole}}{\text{bond length}} \qquad \text{Eq.3.3.6}$$

Interactions between dipoles which have an atom in common, such as O-C-O, are neglected. $C_{sp}3$-H and $C_{sp}3$-$C_{sp}3$ bonds are assumed to have zero bond moments. Partial point charge, δq, assigned are shown in Table 3.3.1.

Table 3.3.1. Partial Point Charges

Reference	bond	length(A)	moment(d)	δq	δq Ax	δq Eq.
42	C-O	1.43	0.4	0.28		
42	O-LP	0.6	0.9	1.5		
41	C-Cl	1.76	1.9	1.08	1.125	1.034
41	C-Br	1.91	1.8	0.942	0.984	0.901

The arrangement of the assigned partial changes are shown in Figure 3.3.1.

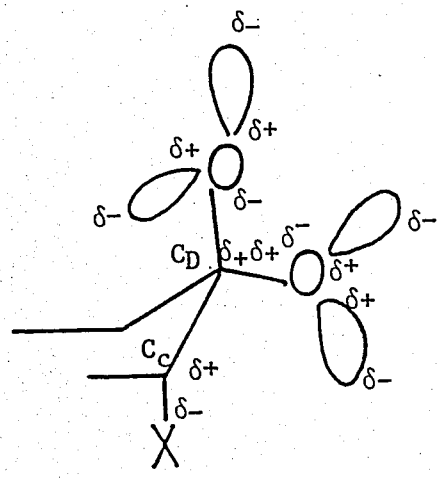

Atom	δq total
LP	-1.5
O	+2.72
C_D	+0.56
C_c	+δq X
X	-δq X

Figure 3.3.1. Arrangement of partial charges.

In Table 3.3.2. all of the dipolar interactions are listed. The interactions which are equivalent in equilibrium I<=>II are shown as "same" and cancel out of the calculations. Since the dipole moments are in Debye units and distances are in Angstrom units in Table 3.3.1, a conversion factor, is required to calculate the electrostatic interactions in kcal/moles. The conversion factor which is calculated as in Eq.3.3.7 is 14.4.

Table 3.3.2. Comparison of atom pairs in equilibrating conformers

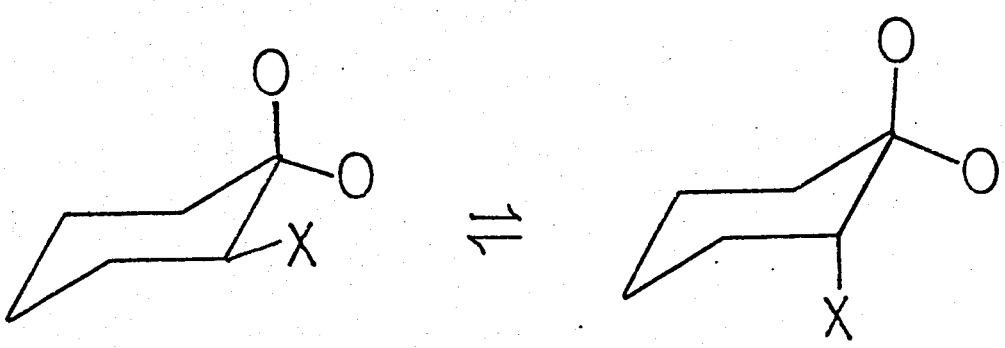

I	II	
2 (X ... O)	2 (X ... O)	different
4 (X ... LP)	4 (X ... LP)	differenet
1 (C_1 ... X)	1 (C_1 ... X)	same*
2 (C_2 ... O)	2 (C_2 ... O)	same
4 (C_2 ... LP)	4 (C_2 ... LP)	same
1 (C_1 ... C_2)	1 (C_1 ... C_2)	same

*They are the same because the distances between the atom pairs remain the same in equilibrating conformers

$$E_{es} \text{ erg/molecule } 6.02\ 10^{23} = E_{es} \text{ erg/mole}$$

$$E_{es} \text{ erg/mole } \frac{1}{4.18\ 10^{10}} = E_{es} \text{ kcal/mole}$$

$$E_{es}\ \frac{D/\mathring{A}\quad D/\mathring{A}}{\mathring{A}} = \frac{\delta q\ \delta q}{r}$$

$$= \frac{10^{-18}\ 10^{-18}}{10^{-24}}\ \frac{6.02\ 10^{23}}{4.18\ 10^{10}} = 14.4 \quad \text{Eq.3.3.7}$$

The electrostatic interactions calculated according to Eq.3.3.5 with dielectric constant D=1 are in Table 3.3.3. and 3.3.4.

Table 3.3.3. Electrostatic Interactions (e.s.u)
Ethylene glycol ketals (I)

		X=Cl	X=Br
I	da=db	-0.953	-0.805
II	dc'	-1.037	-0.879
	dd'	-0.773	-0.651
I	$X\text{-}LP_1$	0.506	0.427
	$X\text{-}LP_2$	0.506	0.427
	$X\text{-}LP_3$	0.432	0.367
	$X\text{-}LP_4$	0.432	0.367
II	$X\text{-}LP_1$	0.635	0.541
	$X\text{-}LP_2$	0.415	0.351
	$X\text{-}LP_3$	0.484	0.414
	$X\text{-}LP_4$	0.384	0.326
I	E_{es} total (kcal/mole)	-0.432	-0.460
II	E_{es} total (kcal/mole)	1.5	1.469

In tables 3.3.3. and 3.3.4. the negative values are attractive and positive values are repulsive. Summation of the electro-

Table 3.3.4. Electrostatic Interactions (e.s.u)
Propylene glycol ketals (2)

		X=Cl	X=Br
I	da=db	-0.953	-0.805
II	dc'	-1.037	-0.879
	dd'	-0.773	-0.651
I	$X-LP_1$	0.487	0.412
	$X-LP_2$	0.487	0.412
	$X-LP_3$	0.437	0.367
	$X-LP_4$	0.437	0.367
II	$X-LP_1$	0.411	0.532
	$X-LP_2$	0.624	0.349
	$X-LP_3$	0.384	0.326
	$X-LP_4$	0.475	0.401
I	E_{es} total (kcal/mole)	-0.835	-0.749
II	E_{es} total (kcal/mole)	1.210	1.123

static interactions show that both systems (1) and (2) have attractive electrostatic interactions for conformer I showing that conformer I is more stable compared to II electrostatically.

3.4. Conformational Free Energy Differences

The conformational free energy difference of the equilibrating conformers I and II may be given by Eq.3.4.1.

$$\Delta E = \Delta E_{vdw} + \Delta E_{es} \qquad \text{Eq.3.4.1}$$

Addition of the results obtained from tables 3.2.2, 3.2.3 to results obtained from tables 3.3.3. and 3.3.4 are tabulated in Table 3.4.1.

Table 3.4.1. Conformational Free Energy Difference

	ΔE^{ax-eq}_{vdw}	$\Delta E^{ax-eq}_{LRvsl,3sAx}$	ΔE^{ax-eq}_{es}	ΔE^{ax-eq}_{total} (kcal/mole)
(1) X=Cl	0.228	1.582	1.93	1.81 + 1.93/D
(1) X=Br	0.354	3.872	1.93	4.23 + 1.93/D
(2) X=Cl	0.241	∿-60	2.04	∿-60
(2) X=Br	0.329	∿-100	1.87	∿-100

From Table 3.4.1. it can be seen that in propylene glycol ketals (2), the substituent will adopt axial conformation II due to the very large long range Van der Waals Interactions that are present in the equatorially oriented substituent I in figure 2.2.2. For ethylene glycol ketals (1) one may say that the conformational free energy difference will be a positive value for various dielectric constant values substituted for D. In Table 3.4.1. ΔG^{ax-eq} positive shows that equatorial oriented conformation will be adopted. That is (1) will have preference for conformer I.

3.5. Comparison of Theoretical Results to those found in the Literature (Experimental Results)

Zefirov et.al.[43] have determined the conformational equilibria of 2-substituted cyclohexanone ketals by NMR. They

have reported that the substituent on ethylene glycol ketals (1) prefer equatorial orientation in contrast to other ketal systems where the substituents display predominance of axial orientation. It has also been reported previously that spiro-compounds containing 5-membered rings show increased amount of equatorially substituted conformers compared with spiroundecane[44]. The conformational data reported by Zefirov et.al.[43] is in Table 3.5.1.

The theoretical results of this work show good agreement with experimental results reported by Zefirov et.al. The preference of an equatorial substituent for ethylene glycol ketals (1) and the preference of an axial substituent for propylene glycol ketals (2) has been shown in both cases.

Table 3.5.1. Experimental Data Reported by Zefirov et.al[43]

Compound	Solvent	% Axial	ΔG_{e-a} kcal/mole	
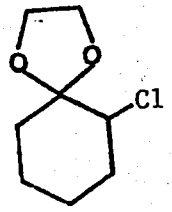	CCl_4	28.4±2.0(19.6±3.6)	-0.56	(-0.85)
	CS_2	21.6±2.0(17.0±0.9)	-0.78	(-0.96)
	C_6H_6	24.5±2.0(20.5±2.7)	-0.68	(-0.81)
	CD_3CN	12.6±2.0(23.2±2.7)	-0.50	(-0.72)
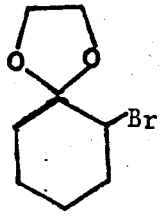	CCl_4	24.5±2.0(18.8±3.6)	-0.68	(-0.88)
	C_6H_6	18.6±2.0(16.1±2.7)	-0.89	(-1.00)
	CD_3CN	25.5±2.0(19.6±3.6)	-0.65	(-0.85)
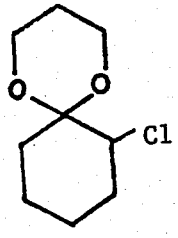	CCl_4	74.5±3.9(57.1±3.6)	0.65	(0.17)
	CS_2	69.6±2.9(52.7±6.3)	0.50	(0.06)
	C_6H_6	71.6±2.9(57.1±0.9)	0.56	(0.17)
	CD_3CN	65.7±2.9(37.5±1.8)	0.39	(0.31)
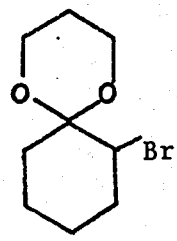	CCl_4	62.8±4.9(51.8±1.8)	0.3	(0.04)
	C_6H_6	57.8±4.9(48.2±4.5)	0.19	(-0.04(-0.04)
	CD_3CN	46.1±3.9(30.4±1.8)	-0.09	(-0.50)

CHAPTER 4

4.1. Application of Molecular Mechanics to 2-nitrocyclohexanone Ketals

The good correlation between theoretical and experimental results found in the literature encourages application of the developed Molecular Mechanics method to 2-nitrocyclohexanone ketals. The nitro group being electronegative could behave like halogens, however both its structure and the presence of the pi-electrons system render it quite different from the halogens. Also by the existence of a charge distribution in the group it gains a totally different character from the halogens. Being composed of three atoms, the nitro group occupies more space. Therefore one may foresee that the nitro group may behave unlike the halogens.

4.2. Description of Model Compounds

The four possible conformers I, II, III, IV of cyclohexanone ethylene ketal(1), and cyclohexanone propylene ketal(2) are the same as shown in figure 2.2.2 and 2.3.2. The X substitutent in this case is the nitro group, everything else being the same.

4.3. Interacting Forces

The interacting forces are similar to those shown for haloketals except that X = NO_2. This group having three atoms increases the number of interactions quantitatively but they are of the same type as listed under 0-2-sübstituent interactions. Therefore important interactions remain to be:

1) 1,1 oxygens and the 2-substituent
2) Lone pairs and the 2-substituent
3) Long range versus syn-axial

The interatomic distances required for the calculations are obtained by constructing Dreiding models and measuring on them. These distances are listed in tables 4.3.1 and 4.3.2 and are shown in figure 4.3.1. Oxygen containing and nitrogen containing interactions have been shown separately in order to avoid overcrowded figures.

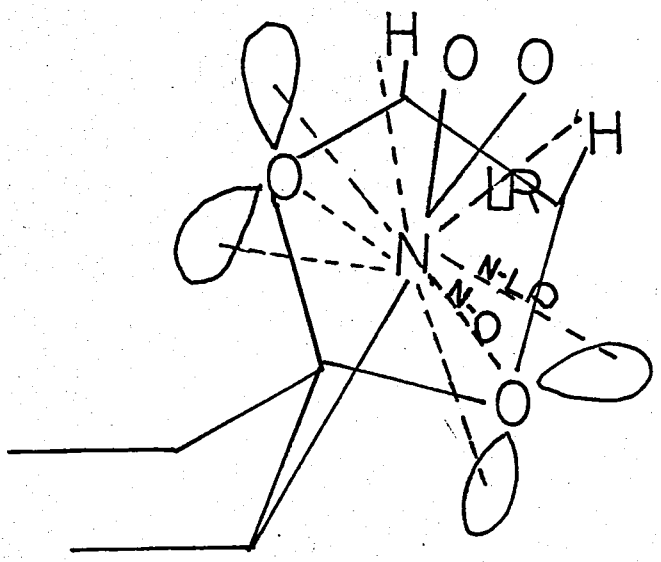

N-O, N-LP, LR interactions

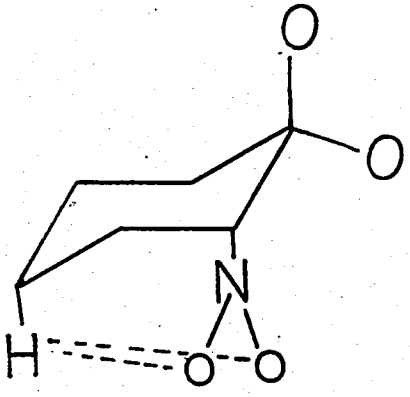

1,3 Syn-Axial interactions

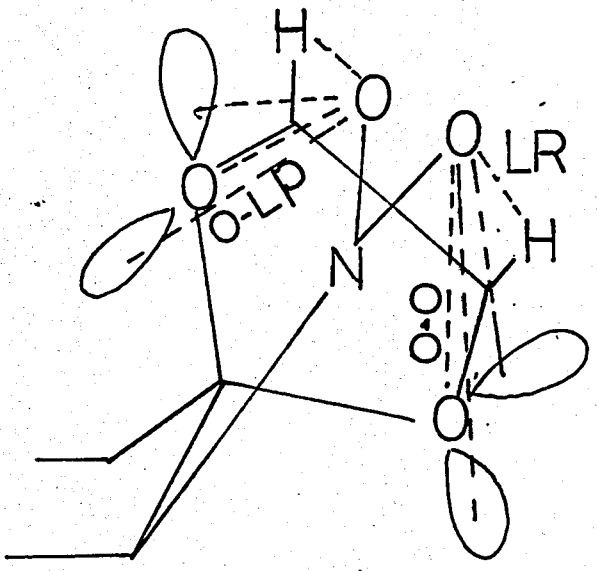

O-O, O-LP, LR interactions

Figure 4.3.1. Interactions for $-NO_2$ group

Table 4.3.1. Intramolecular Distances[a] (Å) for (2)

	I	II	III	IV
$N-O_1$	2.8	2.8	2.8	2.8
$N-O_2$	2.8	3.8	3.8	2.8
$N-LP_1$	3.0	3.9	2.6	2.6
$N-LP_2$	3.0	2.6	3.2	2.6
$N-LP_3$	3.4	4.2	4.0	3.2
$N-LP_4$	3.4	3.4	4.0	3.2
O-O	2.6	3.4	3.2	2.6
O-O	2.6	3.1	3.4	2.6
O-O	4.0	4.1	4.4	4.0
O-O	4.0	4.5	4.4	4.0
O-LP	2.9	4.2	3.4	2.4
O-LP	2.9	4.6	3.8	2.4
O-LP	4.1	3.0	3.0	3.2
O-LP	4.1	3.0	3.0	3.2
O-LP	3.2	4.4	4.6	3.8
O-LP	3.2	4.6	4.6	3.8
O-LP	4.6	5.0	4.2	4.2
O-LP	4.6	5.2	4.8	4.2
Y-O[b]	3.6	3.6	3.6	3.6
Y-O	3.6	4.8	4.8	3.6
Y-LP	3.8	3.2	3.2	3.8
Y-LP	3.8	4.2	4.0	3.8
Y-LP	4.2	5.0	5.0	3.2
Y-LP	4.2	5.2	5.0	3.2

a) Measured from Dreiding models.

b) Y-O, Y-LP are refered to in sec. 4.3.2.

Table 4.3.2. Intramolecular distances* (Å) for (1)

	I	II	III	IV
$N-O_1$	2.8	2.8	2.8	2.8
$N-O_2$	2.8	3.8	3.8	2.8
$N-LP_1$	2.9	2.5	2.8	2.6
$N-LP_2$	3.4	3.8	2.8	3.4
$N-LP_3$	3.4	4.5	4.0	3.4
$N-LP_4$	3.4	4.5	4.0	3.4
O-O	2.6	3.4	3.4	2.6
O-O	2.6	3.0	4.6	2.6
O-O	4.0	4.1	3.4	4.0
O-O	4.0	4.6	4.6	4.0
O-LP	2.8	3.6	3.2	2.2
O-LP	3.9	3.2	3.4	2.2
O-LP	2.8	4.2	3.6	3.4
O-LP	3.9	4.7	3.4	3.4
O-LP	3.0	3.7	4.8	3.6
O-LP	4.5	3.9	5.2	3.6
O-LP	3.0	4.5	4.4	4.4
O-LP	4.5	5.0	4.6	4.4
Y-O	3.6	4.0	4.0	3.6
Y-O	3.6	5.0	5.0	3.6
Y-LP	3.2	3.6	3.7	3.2
Y-LP	3.2	3.4	4.0	3.2
Y-LP	4.4	5.0	5.0	4.2
Y-LP	4.4	5.2	5.0	4.2

*Measured from Dreiding models.

4.4. Steric Interactions

Steric interactions are calculated by Eq. 3.2.1. The new Van der Waals parameters belonging to the nitro substituent are in Table 4.4.1.

Table 4.4.1. Van der Waals Parameters for NO_2[45]

X	r_x^* (Å)	ε_x kcal/moles
N	1.70	0.038
NO_2	1.65	0.046

Van der Waals interactions calculated by Eq. 3.2.1 and with values of Table 4.4.1 are listed in table 4.4.2 and 4.4.3. Similar to halogen counterparts it can be seen from the tables that the largest interactions are long range steric interactions.

Table 4.4.2. Van der Waals Interactions (kcal/moles) for (2)

	I	II	III	IV
N-O	0.030	0.030	0.030	0.030
N-O	0.030	-0.009	-0.009	0.030
N-LP	-0.036	-0.012	-0.035	-0.035
N-LP	-0.024	-0.035	-0.035	-0.035
N-LP	-0.036	-0.008	-0.010	-0.031
N-LP	-0.024	-0.024	-0.010	-0.031
O-O	0.095	-0.012	-0.010	0.095
O-O	0.095	-0.008	-0.012	0.095
O-O	-0.006	-0.006	-0.004	-0.006
O-O	-0.006	-0.003	-0.004	-0.006
O-LP	-0.041	-0.007	-0.021	0.090
O-LP	-0.041	-0.004	-0.014	0.090
O-LP	-0.009	-0.038	-0.038	-0.030
O-LP	-0.009	-0.038	-0.038	-0.030
O-LP	-0.030	-0.005	-0.004	-0.014
O-LP	-0.030	-0.004	-0.004	-0.014
O-LP	-0.004	-0.003	-0.007	-0.007
O-LP	-0.004	-0.002	-0.003	-0.007
LR O-H	>200	2.354	2.354	-0.047
LR N-H		0.040	0.040	-0.012
Evdw total	>200	4.6	4.56	0.062

Table 4.4.3. Van der Waals Interactions (kcal/moles) for (1)

	I	II	III	IV
N-O	0.030	0.030	0.030	0.030
N-O	0.030	-0.009	-0.009	0.030
N-LP	-0.038	-0.034	-0.036	-0.035
N-LP	-0.024	-0.026	-0.036	-0.024
N-LP	-0.038	-0.013	-0.025	-0.035
N-LP	-0.024	-0.005	-0.010	-0.024
O-O	0.095	-0.012	-0.012	0.095
O-O	0.095	-0.008	-0.003	0.095
O-O	-0.006	-0.006	-0.012	-0.006
O-O	-0.006	-0.003	-0.003	-0.006
O-LP	-0.039	-0.018	-0.030	0.429
O-LP	-0.011	-0.030	-0.021	0.429
O-LP	-0.039	-0.007	-0.018	-0.021
O-LP	-0.011	-0.004	-0.021	-0.021
O-LP	-0.039	-0.016	-0.003	-0.018
O-LP	-0.005	-0.011	-0.002	-0.018
O-LP	-0.039	-0.005	-0.005	-0.005
O-LP	-0.005	-0.003	-0.004	-0.005
LR O-H	39.46	15.604	15.604	-0.060
LR N-H	1.052	2.196	2.196	0.017
Evdw total	~80	35.42	35.41	0.765

The sum of Van der Waals Interactions for both (1) and (2) in Tables 4.4.2 and 4.4.3 show that there is almost no difference between the axially oriented conformer II and III sterically but a large difference between the equatorially oriented conformers I and IV. The magnitude of the steric interactions show that conformer I does not exist. Therefore conformer IV being the most stable, is prefered.

4.5. Electrostatic Interactions

The electrostatics of the nitro group consists of charge-dipole and dipole-dipole interactions, due to the presence of formal charges. The electrostatic interactions are calculated according to Eq. 3.3.5 with dielectric constant D=1 and with conversion factor 14.4 according to Eq. 3.3.7. Partial point charges are assigned as in Section 3.3 and are shown in Figure 4.5.1 and 4.5.2.

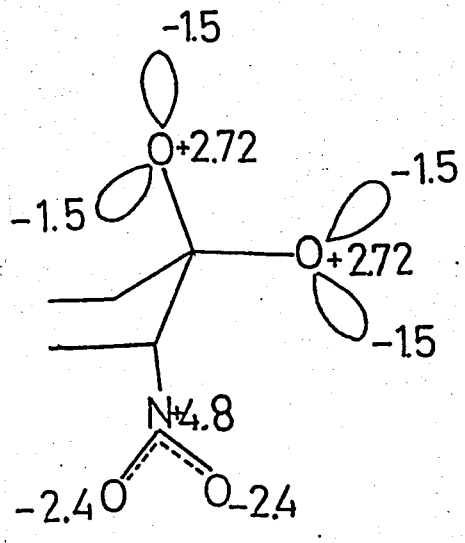

Figure 4.5.1. Charge-dipole interactions

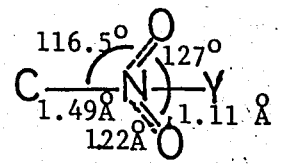

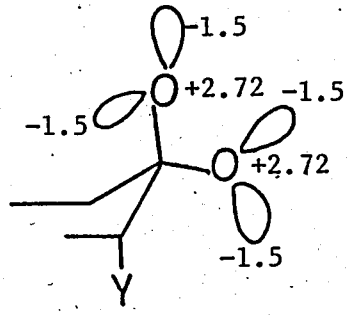

Y	$\frac{\delta qAx}{1.38}$	$\frac{\delta qEq}{1.32}$ (46)

Figure 4.5.2. Dipole-dipole interactions

In figure 4.5.1, the assignment of the formal charges on the nitro group is shown. In figure 4.5.2, the assignment of a partial point charge due to the nitro group dipole is shown. In figure 4.5.2, the negative end of the C-NO_2 dipole is shown as the point Y. The C-Y distance is chosen to be 2.6 Å. This locus for point Y is assigned by trial and error method to fit best with experimental data. The dipole moment of the nitro group is taken to be 3.5 D[46] and the partial point charge is assigned by Eq. 3.3.6. The calculated electrostatic interactions according to Eq. 3.3.5 are in tables 4.5.1, 4.5.2, 4.5.3 and 4.5.4.

Table 4.5.1. Charge-dipole Electrostatic Interactions (e.s.u.) Propylene Glycol Ketal (2)

	I	II	III	IV
N-O	4.66	4.66	4.66	4.66
N-O	4.66	3.43	3.43	4.66
N-LP	-2.38	-1.87	-2.77	-2.77
N-LP	-2.38	-2.77	-2.25	-2.77
N-LP	-2.11	-1.73	-1.80	-2.25
N-LP	-2.11	-2.11	-1.80	-2.25
O-O	-2.51	-1.92	-2.04	-2.51
O-O	-2.51	-2.11	-1.92	-2.51
O-O	-1.63	-1.59	-1.48	-1.63
O-O	-1.63	-1.42	-1.48	-1.63
O-LP	1.24	1.50	1.06	1.50
O-LP	1.24	0.78	0.95	1.50
O-LP	0.88	1.20	1.20	1.13
O-LP	0.88	1.16	1.20	1.13
O-LP	1.13	0.82	0.78	0.95
O-LP	1.13	0.82	0.78	0.95
O-LP	1.13	0.78	0.78	0.95
O-LP	0.78	0.72	0.86	0.86
O-LP	0.78	0.69	0.75	0.86
$E_{charge-dip}$ (kcal/mole)	1.73	3.17	1.87	-1.73

Table 4.5.2. dipole-dipole Electrostatic Interactions (e.s.u.) Propylene Glycol Ketals (2)

	I	II	III	IV
Y-O	-1.00	-1.04	-1.04	-1.00
Y-O	-1.00	-0.78	-0.78	-1.00
Y-LP	0.52	0.65	0.65	0.52
Y-LP	0.52	0.49	0.52	0.52
Y-LP	0.47	0.41	0.41	0.62
Y-LP	0.47	0.40	0.41	0.62
$E_{dip-dip}$ (kcal/mole)	-0.29	1.87	2.45	4.03

Table 4.5.3. charge-dipole Electrostatic Interactions Ethylene glycol Ketals (1) (in e.s.u)

	I	II	III	IV
N-O	4.66	4.66	4.66	4.66
N-O	4.66	3.43	3.43	4.66
N-LP	-2.48	-2.88	-2.57	-2.77
N-LP	-2.12	-1.85	-2.57	-2.12
N-LP	-2.48	-2.18	-1.95	-2.77
N-LP	-2.12	-1.60	-1.80	-2.12
O-O	-2.51	-1.92	-1.92	-2.33
O-O	-1.63	-2.18	-1.42	-2.33
O-O	-2.51	-1.59	-1.92	-1.63
O-O	-1.63	-1.42	-1.42	-1.63
O-LP	1.29	1.00	1.13	1.64
O-LP	0.92	1.13	1.06	1.64
O-LP	1.29	0.86	1.00	1.06
O-LP	0.92	0.77	1.06	1.06
O-LP	1.20	0.97	0.75	1.00
O-LP	0.80	0.92	0.69	1.00
O-LP	1.20	0.80	0.82	0.82
O-LP	0.80	0.72	0.78	0.82
$E_{charge-dip}$ (kcal/mole)	3.74	-.576	-2.74	9.50

Table 4.5.4. dipole-dipole Electrostatic Interactions Ethylene glycol Ketals (in e.s.u) (1)

	I	II	III	IV
Y-O	-1.00	-1.04	-1.04	-1.00
Y-O	-1.00	-0.78	-0.78	-1.00
Y-LP	0.58	0.31	0.61	0.62
Y-LP	0.58	0.52	0.58	0.62
Y-LP	0.45	0.41	0.41	0.47
Y-LP	0.45	0.40	0.40	0.47
$E_{dip-dip}$ (kcal/mole)	0.86	-2.59	2.59	2.59

Table 4.5.5. Total Electrostatic Interactions (kcal/mole)

	I	II	III	IV
(2) charge-dipole	1.73	3.17	1.87	-1.73
(2) dip-dipole	-0.29	1.87	2.45	4.03
(2) E_{es} total	1.44	5.04	4.32	2.30
(1) charge-dipole	3.74	-5.76	-2.74	9.50
(1) dip-dipole	0.86	-2.59	2.59	2.59
(1) E_{es} total	4.60	-8.35	-0.15	12.09

For propylene glycol ketal system (2), one can observe from Table 4.5.1 that charge-dipole interactions are attractive for conformer IV and repulsive for the other conformers. In Table 4.5.2 the dipole-dipole interactions show to be attractive for conformer I. The total electrostatic interactions in Table 4.5.5 show preference for conformer I.

For ethylene glycol system (1), one can observe from Table 4.5.3 the charge-dipole interactions are attractive for conformers II and III. In table 4.5.4 the dipole-dipole interactions show to be attractive only for conformer II. Total electrostatic interactions in Table 4.5.5 show preference for conformer II.

4.6. Conformational Free Energy Difference

The conformational free energy difference of the equilibrating conformers can be given as in Eq. 3.4.1. In Table 4.6.1 and 4.6.2 one may find the sums of the Tables 4.4.2, 4.4.3, 4.5.1, 4.5.2, 4.5.3, 4.5.4. Each type of interaction contributing to the total energy is shown separately. In Table 4.6.1 one observes that the largest value contributing to the total energy is the long-range steric interactions. Conformer I has the largest value due to the very crowded interactions as seen in Figure 4.6.1. The nitro group is almost lieing on the dioxane ring. therefore a very high value for long range steric interactions is observed.

Table 4.6.1. Conformational Free Energy for (2) (kcal/mole)

(2)	I	II	III	IV
E_{vdw}	0.050	-0.188	-0.228	0.184
E_{es} (D=1)	1.44	5.04	4.32	2.30
$E_{1,3}$ vs LR	>200	4.79	4.79	-0.118
E_{total}	>200	9.6	8.89	2.37

Table 4.6.2. Conformational Free Energy for (1) (kcal/mole)

(1)	I	II	III	IV
E_{vdw}	-0.074	-0.180	-0.181	0.851
E_{es} (D=1)	4.60	-8.35	-0.15	12.09
$E_{1,3}$ vs LR	∿80	∿35	∿35	-0.086
E_{total}	∿84.5	∿27	∿35	12.85

This clearly demonstrates that conformer I is not possible. In contrast, conformer IV in figure 4.6.1 is highly probable because the nitro group is far apart from the hydrogens shown. Similarly from table 4.6.1 it can be observed that the difference in energy between conformer II and III mainly arises from electrostatic interactions. These can be seen in figure 4.6.2 where the dipoles created by the presence of the ketal ring are directed towards the nitro group in III whereas they are directed away from the nitro group in II. Therefore, one observes that conformer II and IV are of lowest energy in (2) and their differences in energy

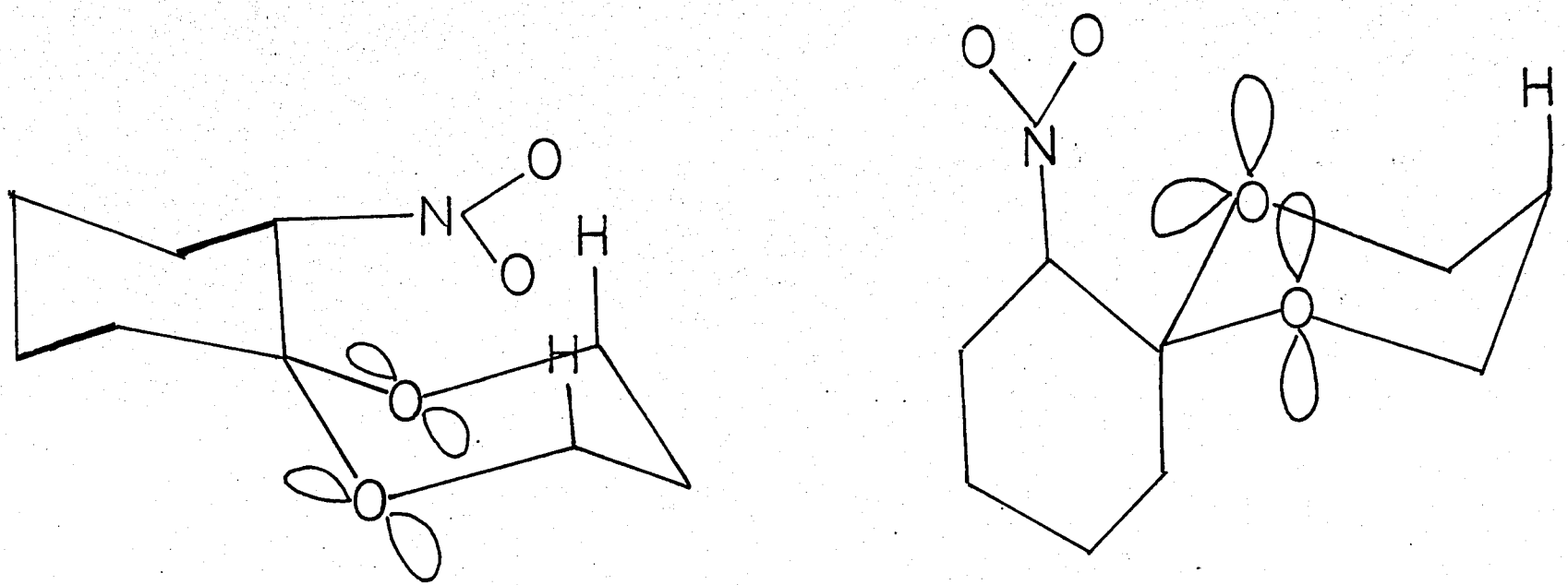

Figure 4.6.1. Long range interactions in conformer I and IV

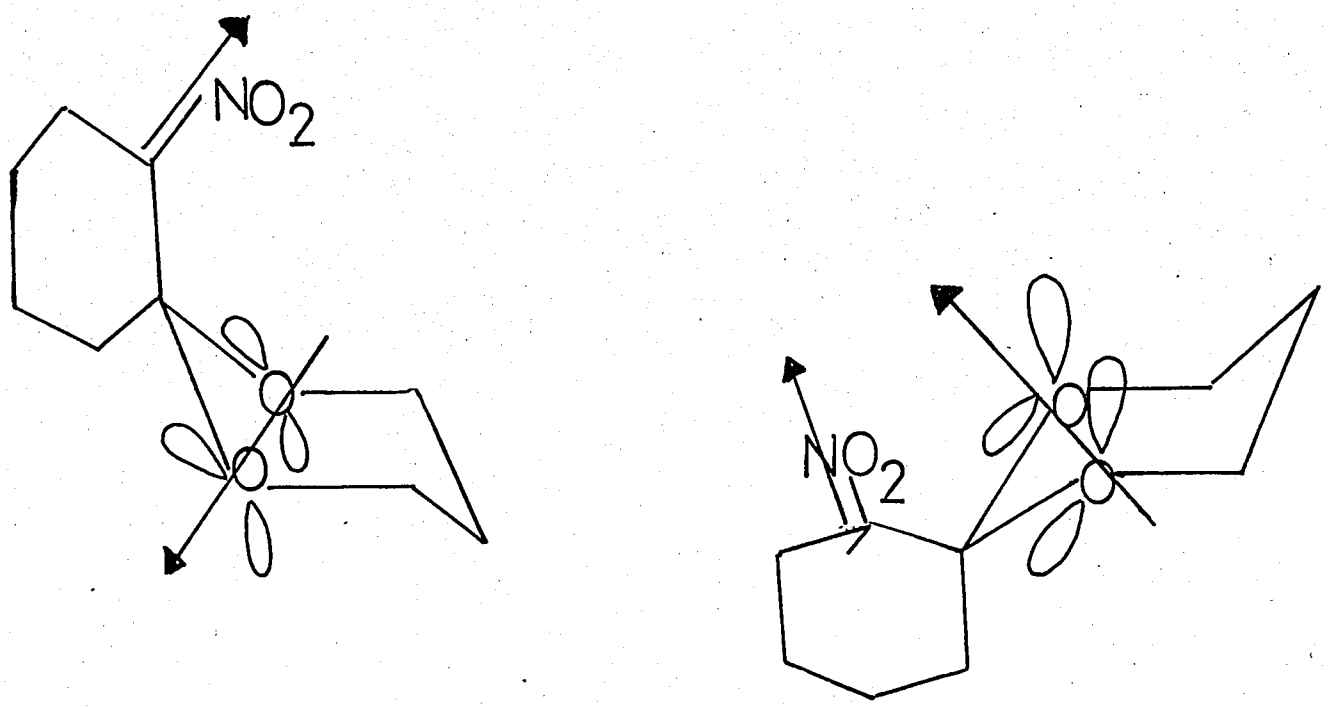

Figure 4.6.2. Electrostatic interactions in conformers II and III

is considered as the conformational free energy difference. According to results obtained from Table 4.6.1, (2) ΔG^{ax-eq} = ∿7.5 kcal/mole. In other words (2) prefers to exist in the form of IV by 7.5 kcal/mole compared to II.

In Table 4.6.2 for (1) it can be seen that II and IV are of lowest energy as in (2). Similarly the largest value contributing to total energy is the long range interactions which is greatest for I and least for IV. Electrostatic interactions in Table 4.6.2 are more attractive for conformer II than conformer III. This is a result of different directions of the dipoles created by the ketal ring oxygens. They have an opposite direction to that of the nitro group in II whereas they are directed towards the nitro group in III. Therefore conformers II and IV are of lowest energy in (1) and according to results obtained from Table 4.6.2, (1) ΔG^{ax-eq} = ∿15 kcal/mole. (1) similar to (2) prefers conformation with equatorial nitro group (IV).

The results of Table 4.6.1 are evaluated in the manner of

$$\Delta G^{ax-eq} = E(II) - E(IV) \qquad \text{Eq 4.6.1}$$

Where E's are the calculated energies of the conformers. Substituting the sum of all energy components in Table 4.6.1 along with dielectric constant D, Eq. 4.6.2 is obtained.

$$(2)\ \Delta G^{ax-eq} = 4.68 + 2.74/D \qquad \text{Eq 4.6.2}$$

Then ΔG^{ax-eq} for (2) can be evaluated at different solvents by Eq. 4.6.2. The same treatment for (1) is given as

$$(1)\ \Delta G^{ax-eq} = 35 - 20/D \qquad \text{Eq. 4.6.3}$$

by substituting the sum of all energy components in Table 4.6.2. The free energy differences computed in different solvents are listed in Table 4.6.3.

Table 4.6.3. Conformational Free Energy Difference in Different Solvents

Solvent	D	(2) ΔG^{ax-eq} kcal/mole	(1) ΔG^{ax-eq} kcal/mole
CCl_4	2.24	5.9	26
$CHCl_3$	4.81	5.25	31
Acetone	20.7	4.81	34

From Table 4.6.3 it can be seen that the dielectric constant will change ΔG^{o} to some extent but the conformers will still remain in the conformation where the substituted nitro group is equatorially oriented.

CHAPTER 5

5.1. Application of NMR Parameters to Conformational Study of 2-nitrocyclohexanone Ketals

There are several experimental methods of conformational analysis. These are dipole moments, dissociation constants, ORD curves, I.R., U.V and N.M.R spectra[47]. NMR is one of the best methods available for the conformational analysis of cyclohexane derivatives[48] since a number of parameters such as coupling constants, band widths and chemical shifts can be used. The cyclohexane system is particularly suitable for studies of conformational equilibria as it posesses two favorable conformations which correspond to the two chair forms of cyclohexane, figure 2.2.1.

The computation of conformational free energies for mobile systems require the NMR parameters of specific protons of conformers to be determined individually. At room temperature, the interconversion between the two chair conformations of cyclohexane is much faster than the relaxation time observed for the protons. Thus the NMR spectrum of

such a flexible system is the average of the two conformations. If the interconversion can be slowed down or stopped, the NMR spectrum of both conformers can be observed. This can be accomplished in two ways. When the NMR spectrum of a cyclohexane derivative is cooled down to about -80°C, the ring interconversion is slowed down so that both conformational parameters can be determined individually[49]. However this method has certain experimental difficulties[50].

A more frequently employed method is the use of model compounds which are very similar to conformers being examined but, which can not interconvert. Winstein and Holness introduced the use of t-butyl group as an anchor for holding conformation[51]. From the NMR spectra of such a 4-t-butyl analogue of the compound under investigation the necessary parameters for the pure equatorial and pure axial conformers can be determined.

In the NMR spectrum it is possible to distinguish between different types of protons which absorb at different fields. The hydrogen on the same carbon as the substituent is called the α-proton. Since most common substitutents are more electronegative than a methylene unit and exert a deshielding effect on the α-proton, the α-proton generally appears at lower field than other ring protons[52]. For this reason α-proton signals are of particular value in conformational analysis. The NMR parameters that can be used to evaluate the α-proton signal are

1- the chemical shift

2- the band width

3- the coupling constant

Equational and axial protons resonate at different field strengths. In general an equatorial α-proton will absorb at a lower field than the axial one[53]. Depending on the nature of the substituent, chemical shift values may differ from 0.1 to 0.7 ppm. Coupling constants depend on dihedral angles between protons on adjacent carbon atoms[54]. In addition to angle dependency, vicinal coupling depends also on electronegativity of the substituents, C-C-H bond angles, and bond lengths. However, effects other than dihedral angles are small. Theoretical treatments by Karplus[54] express coupling constant, J, by equations 5.1.1 and 5.1.2

$$J = J^{o} \cos^{2} \phi - C \quad (0^{o} \leq \phi \leq 90^{o}) \qquad \text{Eq 5.1.1}$$

$$J = J^{180} \cos^{2} \phi - C \quad (90^{o} \leq \phi \leq 180^{o}) \qquad \text{Eq 5.1.2}$$

Where $J^{o} = 8.5$ Hz; $J^{180} = 9.5$ Hz and $C = -0.3$ Hz are constants. The use of coupling constants for conformational analysis has been published by Booth[55] and applied succesfully to various monosubstituted cyclohexane systems. In the case of ethylene and propylene ketals of 2-nitrocyclohexanone, (1) and (2), only two protons couple with α-proton. Considering equilibrium in figure 2.2.1 where (X) represent mole fraction of equatorial conformer and (1-X) represents mole fraction of axial conformation. The average coupling

constants $J_{H_\alpha H_1}$ and $J_{H_\alpha H_2}$ of the α-proton can be expressed by Eq. 5.1.3 and Eq. 5.1.4

$$J_{H_\alpha H_1} = (X)\, J_{ae} + (1-X)\, J_{ee} \qquad \text{Eq. 5.1.3}$$

$$J_{H_\alpha H_2} = (X)\, J_{ae} + (1-X)\, J_{ea} \qquad \text{Eq. 5.1.4}$$

The band width parameter is the sum of the coupling constants which cause the splitting in the NMR signal of the proton under investigation; and is measured between the outer lines of the multiplet. Band width parameter is independent of spectrum order therefore even if an α-proton signal is completely unresolved it is possible to measure the band width at a predetermined height. For such cases, generally the band width measured at half height (1/2 W) have been utilized.

Starting with the expression relating the conformational rate constant K in the form of Eq. 5.1.5, the free energy difference ΔG between the conformers is given by Eq. 5.1.6.

$$K = \frac{P_a - P}{P - P_e} \qquad \text{Eq. 5.1.5}$$

In Eq. 5.1.5 P_a and P_e are the magnitudes of a property of a rigid (unflexible) molecule with an axial and an equatorial functional group, respectively. P is the measured value of this property in the flexible system.

$$\Delta G = -RT\ln K \qquad \text{Eq. 5.1.6}$$

In Eq. 5.1.6, R is 1.987 cal/mole. The systems under investigation spiro-[5,4]-1-nitro-6,9-dioxodecane (1), Fig. 5.1.1 and spiro-[5,5]-1-nitro-6,10-dioxoundecane (2), Fig. 5.1.2 and their 4-t-buty analogues Fig. 5.1.3 have been synthesized as described in chapter 6. A complete scheme of synthesis is shown in Fig. 6.1.1. The NMR parameters of the α-protons for the ketal systems (1) and (2) are listed in Table 5.1.1.

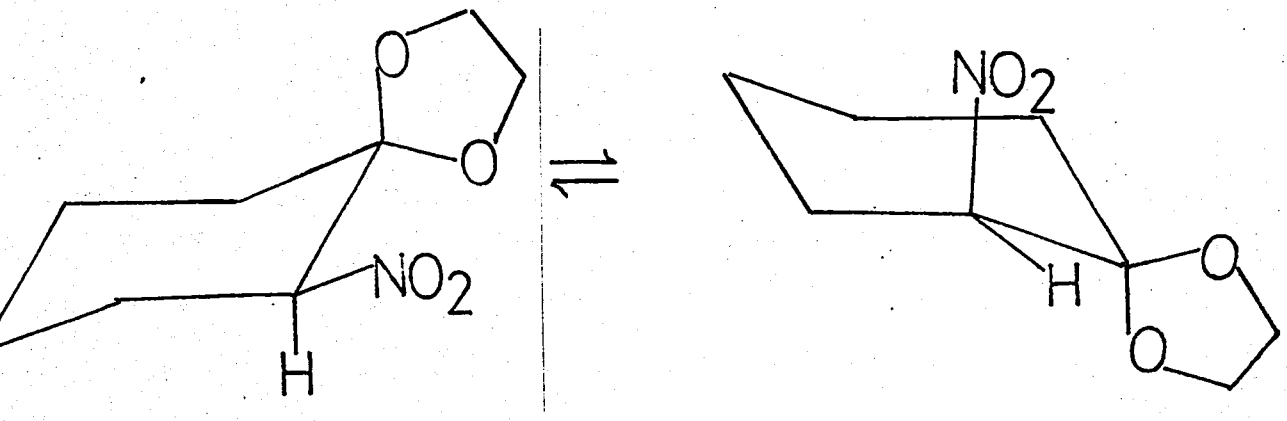

Figure 5.1.1. α-proton inversion in (1)

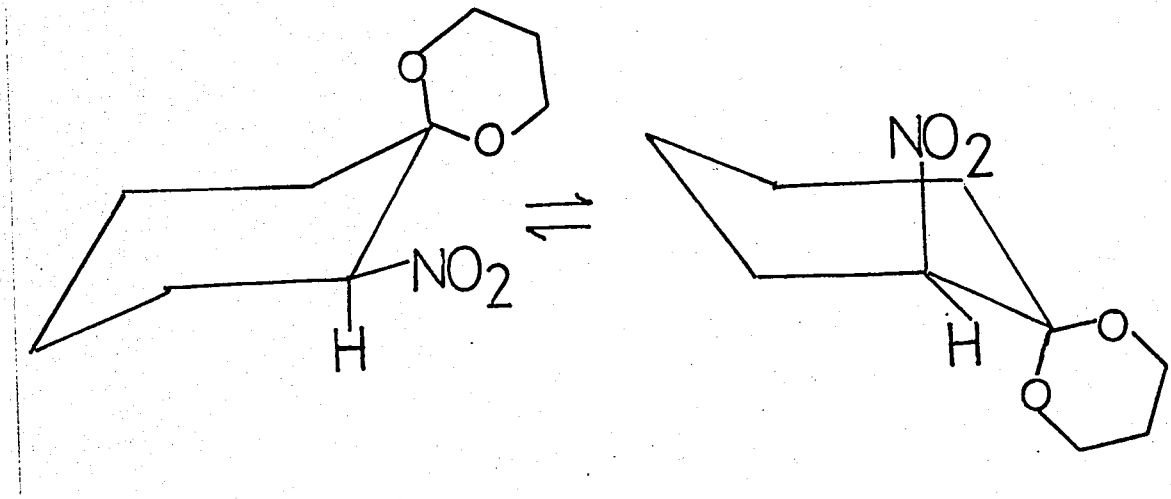

Figure 5.1.2. α-proton inversion in (2)

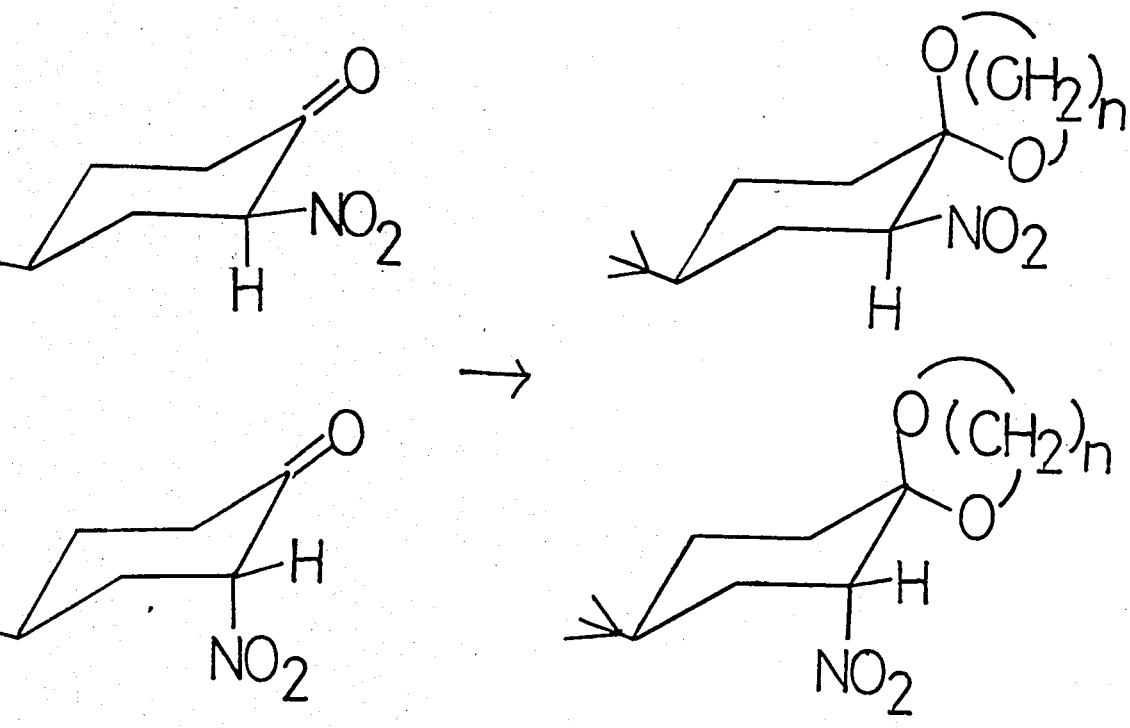

Figure 5.1.3. 4-t-butyl analogues of (1) and (2)

Table 5.1.1. α-Proton Signals (in CCl_4, 200 MHz NMR)

	α-H (ppm)	width (Hz)	ref. to spectra
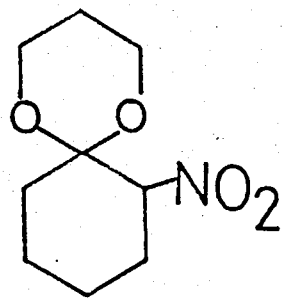	4.76	12.6	81
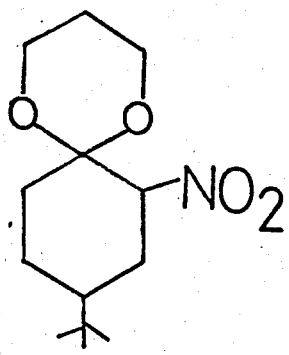	4.565	13	83
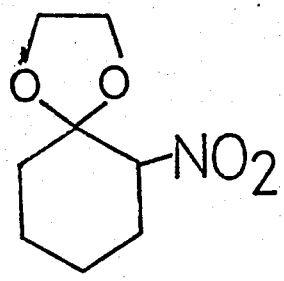	4.6	16.8	76
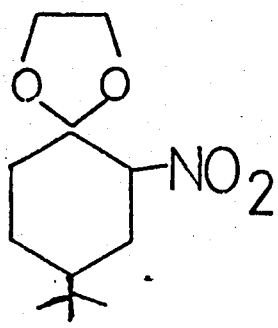	4.16 4.63	9 17	79

As can be seen from Table 5.1.1, (2) flexible system gives an α-proton signal nearer to the signal belonging to the conformer bearing the equatorial nitro group. Also the width of the α-proton of the anchored (2) system with an equatorial substituent. These indicate that (2) prefers a conformation where the nitro group is equatorially oriented. Evaluation of the α-proton parameters of the (1) system shows that the α-proton signals do not resemble to that of simple cyclohexane derivatives. Instead, they resemble the characteristics of an α-proton of cyclohexanone[56] systems.

In this system (cyclohexanone), the axial α-proton absorbs at a lower field than the equatorial α-proton[57]. The α-proton of the flexible (1) system gives a signal nearer to the signal at lower field obtained for the rigid (1) system with equatorial nitro group. Also the width of the α-proton signal for flexible (1) system resembles to that of the rigid (1) system with equatorial nitro group. One can easily deduce that (1) system prefers to have conformation where the nitro group is equatorially oriented. The difference in conformational free energies for (1) and (2) systems has been calculated by using Eq. 5.1.6 and Eq. 5.1.5. P in Eq. 5.1.5 has been used as band width (W) from Table 5.1.1.

(1) $\Delta G = 2.132$ cal/mole

(2) $\Delta G = 1.536$ cal/mole

When P in Eq. 5.1.5 has been used as chemical shift (δ)

from Table 5.1.1 than ΔG values are

(1) $\Delta G = 1.576$ cal/mole

(2) $\Delta G = 0.556$ cal/mole

In both cases both system (1) and (2) show preference for equatorial conformer. The nitro group showing an equatorial preference both in (1) and (2) exhibits a behavior that is opposite to those of halogens. Halogens show equatorial preference only in (1) and axial preference in (2) and other ketal systems[58]. This kind of anomalous behavior for the nitro group is also observed by Eliel et.al[59]. They report nitro to adopt axial conformation in contrast to halogens in 5-hetero-substituted-2-isopropyl-1,3-dioxanes. Zajac and Özbal[60] report that though the halogens on 2-halocyclohexanones prefer axial conformation, the nitro group on 2-nitrocyclohexanone adopts equatorial conformation. They explain the origin of this behavior in the attractive electrostatic interaction of the polar nitro and carbonyl groups. In all of the cases mentioned above one observes a parallel behavior of the nitro group.

Comparison of experimental results with theoretical results show that they agree in conformational preference. Both theoretical and experimental results determine (1) and (2) to adopt equatorial conformation, Table 5.1.2. But the theoretical results are higher in value than that of experimental results. This difference may arise due to "special conformational effects"[61].

Table 5.1.2. Theoretical and Experinatal Results for Systems (1) and (2)

	(1)	(2)
ΔG (W)*	2.132	1.536
% Eq (W)	97	93
ΔG (δ)*	1.576	0.556
% Eq (δ)	94	72
ΔG (MM)*	35	4.68
% Eq (MM)	100	100

*The method used (i.e.: width, chemical shift parameters; molecular mechanics) showed in parantheses.

CHAPTER 6

6.1. Synthesis

The systems under investigation spiro-[5,4]-1-nitro-6, 9-dioxodecane (1), Fig. 5.1.1 and spiro-[5,5]-1-nitro-6,10 - dioxoundecane (2), Fig. 5.1.2 and their 4-t-butyl analogues Fig. 5.1.3 have been synthesized. A complete scheme of synthesis is shown in Fig. 6.1.1.

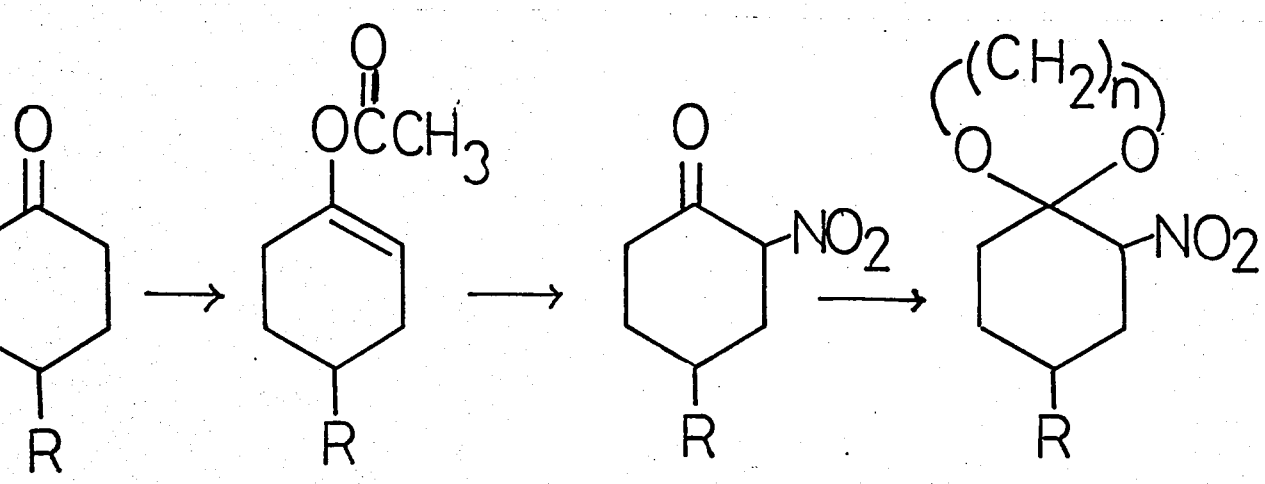

Figure 6.1.1. Scheme of synthesis

In figure 6.1.1, the enol acetate of cyclohexanone was prepared with acetic anhydride[62], Nitration of the enol acetate was accomplished by acetyl nitrate[63]. Both methods have been reported in the literature. Synthesis of the ketal

required some effort to find optimum reaction medium, temperature and time. After trial of various solvents acetonitrile proved to be a suitable solvent and best yields were found to be obtained after a reaction time of 4 to 6 hours at 70 to 75°C. Other solvents were not satisfying because they didn't solvate both the glycol and the 2-nitrocyclohexanone. 2-nitrocyclohexanone being susceptible to acidic and basic media and to high temperatures decomposed to give low yields. However the pure ketals obtained, though at low yields gave satisfactory elementary analysis results.

6.2. Equipment, Reagents and Starting Materials

Varian HA200 MHz NMR was used for spectra. Elementary analysis were done by Galbraith Laboratories, Inc. Knoxville, Tennessee.

Commercial Reagents:

1- Acetic anhydride
2- Ethylene glycol
3- Propylene glycol
4- P-Toluene sulfonic acid
5- Nitric acid
6- Potassium carbonate
7- Sodium bicarbonate
8- (anhy.) Magnesium sulfate
9- Acetonitrile
10- Carbontetrachloride

11- Deutrochloroform

12- Acetone (d_6)

13- TMS

14- Ether

Starting Materials:

1- Cyclohexanone

2- 4-t-butyl-cyclohexanol

6.3. 4-t-butylcyclohexanone

A mixture of 100 g (0.641 mole) of 4-t-butylcyclohexanol, 32 ml conc. H_2SO_4 and 192 ml H_2O was placed in a 2000 ml beaker and cooled in an ice-water bath. To this mixture, a solution of 95 g (0.32 mole) $K_2Cr_2O_7$ dissolved in 350 ml H_2O and 44.8 ml H_2SO_4 was added dropwise over a period of 3 hours with constant stirring. After the addition was complete, the solution was heated to 100°C for 1 hr. and left at room temperature overnight. The white-green organic solid that was formed was removed from the container and the remaining solution was extracted with ether two times with 200 ml portions. The extracts were used to dissolve the organic solid. The solution was then washed with 5 % aqueous K_2CO_3 and 5 % aqueous $NaHCO_3$ then dried over anhydrous $MgSO_4$ and concentrated.

6.4. 1-Acetoxycyclohexene (Enol Acetate of Cyclohexanone)

A mixture of 98.0 g (1.0 mole) of cyclohexanone, 204.0 g (2.0 mole) of acetic anhydride and 1.0 g of p-toluenesulfonic acid was placed in a 500 ml round-bottom flask, equipped with a magnetic stirrer and a condenser. The mixture was refluxed for four hours. After it was cooled to room temparature it was washed several times with water, 5 % K_2CO_3 and water again. Some saturated salt solution was used to break emulsion. The crude product was distilled through 6" Vigreux column and four fractions were collected. Fraction four was pure enol acetate. Fractions two and three were combined and redistilled and three fractions were collected. Fractions two and three were pure enol acetate.

6.5. 1-Acetoxy-4-t-butylcyclohexene (Enol Acetate of 4-t-butylcyclohexanone)

A mixture of 39 g (0.275 mole) of 4-t-butylcyclohexanone, 115 g (1.1 mole) of aceticanhydride and 0.1 g of p-toluenesulfonic acid was refluxed for 15 hours in a 250 ml round-bottom flask equipped with a magnetic stirrer and a condenser. The clear solution was cooled to room temperature and partitioned between pentane and 5 % K_2CO_3. The organic layer was separated, washed with saturated salt solution, dried over anhydrous $MgSO_4$ and concentrated. The remaining yellow liquid was distilled through a 6" Vigreux column. Three fractions were collected. Fraction two and three were pure enol acetate.

6.6. 2-nitrocyclohexanone

A mixture of 79 g (0.56 moles) of 1-Acetoxycyclohexene and 175 g (1.71 moles) of acetic anhydride was placed in a 3-neched 500 ml round bottom flask equipped with a magnetic stirrer and a thermometer. 39 ml (0.56 moles) of conc. HNO_3 was added dropwise to the stirred solution and the temperature of the solution was kept between 18-20°C. The solution was stirred at 18-20°C for 1hr after acid addition was completed. The solution was then transferred to a vacuum distillation apparatus, and the residual acetylnitrate, acetic acid and excess acetic anhydride were removed. The remaining liquid crystallized upon standing in the freezer. Than treated for ketal formation.

6.7. 2-nitro-4-t-butylcyclohexanone

A mixture of 8.85 g (0.045 mole) of 1-Acetoxy-4-t-butylcyclohexene and 14 g (0.135 mole) of acetic anhydride was placed in a 3-necked 100 ml round bottom flask equipped with a magnetic stirrer and a thermometer. 3.17 ml (0.05 moles) of conc. HNO_3 was added dropwise to the stirred solution and the temperature was kept at 18-20°C. The solution was stirred for 1 hr at 18-20°C after addition of acid was complete. The residual acetylnitrate, acetic acid and excess acetic anhydride were removed under reduced pressure. The remaining liquid was immediately treated for ketal formation.

6.8. Ethylene ketal of 2-nitrocyclohexanone

5 g of 2-nitrocyclohexanone (0.035 mole), 5.75 g (0.093 mole) of 1,2-Ethylene diol and a few crystals of P-toluene-sulfonic acid was dissolved in 50 ml acetonitrile. The mixture was placed in a 100 ml round bottom flash equipped with a magnetic stirrer and (75°C) refluxed hour hours. After cooling to room temperature the crude product was partitioned between water and ether. Ether layer was weshed several times with aqueous 5 % $NaHCO_3$ and water than dried over anhydrous $MgSO_4$. The remaining viscous liquid crystallized in CCl_4 in the freezer (-18°C). Anal: calcd. for $C_8H_{13}NO_4$: C, 51.33; H, 6.95; N, 7.48; Found: C, 51.40; H, 7.06; N, 7.33. NMR (CCl_4 (ppm)): 4.6 (q, α proton), 3.9 (s, ketal ring protons), 2.4-1.2 (m, ring protons).

6.9. Ethylene ketal of 2-nitro-4-t-butylcyclohexanone

8.0 g (0.043 moles) of 4-t-butylcyclohexanone, 8.0 g (0.129 moles) of 1,2-ethanediol and a few crystals of p-toluene sulfonic acid was dissolved in 50 ml acetonitrile. The mixture was placed in a 100 ml round bottom flash equipped with a magnetic stirrer and refluxed for 6 hrs (at ∿75°C). After cooling to room temparature the crude product was partitioned between water and ether. The ether layer was washed several times with aqueous 5 % $NaHCO_3$ and water, than dried over anhydrous $MgSO_4$. The remaining liquid crystallized in CCl_4 in the freezer (-18°C). Anal: calcd. for $C_{12}H_{21}NO_4$: C, 59.25;

H, 8.64; N, 5.76; Found: C, 63.44; H, 8.95; N, 1.71; NMR (CCl_4(ppm)): 4.16 (α proton), 4.63 (α proton), 3.98 (s, ketal ring proton) 0.94 (d, t-bu protons), 2.4-1.2 (m, ring protons).

6.10. Propylene ketal of 2-nitrocyclohexanone

5 g of 2-nitrocyclohexanone (0.035 mole), 7.6 g (0.1 mole) 1,3-propylene diol and a few crystals of pTSA was dissolved in 50 ml acetonitrile. The mixture was placed in a 100 ml round bottom flask equipped with a magnetic stirrer and refluxed for four hours at ∿75°C. After cooling to room temperature the crude product was partitioned between water and ether. Ether layer was washed several times with aqueous 5 % $NaHCO_3$ and water then dried over anhydrous $MgSO_4$. Remaining liquid crystallized in CCl_4 in the freezer (-18°C). Anal: calcd. for $C_9H_{15}NO_4$: C, 53.73; H, 7.46; N, 6.97; Found: C, 57.79: H, 8.23; N, 6.02 NMR (CCl_4 (ppm)): 4.76 (q, α-proton), 3.98 (m, ketal ring protons), 2.8-0.9, (m, ring protons).

6.11. Propylene ketal of 2-nitro-4-t-butylcyclohexanone

8 g (0.043 roles) of 4-t-butylcyclohexanone, 9.1 g (0.12 moles) of 1,3-propanediol and a few crystals of pTSA was dissolved in 50 ml acetonitrile. The mixture was placed in a 100 ml round bottom flask equipped with a magnetic stirrer and refluxed for six hours (∿75°C). After cooling to room temperature the crude product was partitioned between

water and ether. The ether layer was washed several times with aqueous 5 % $NaHCO_3$ and water, than dried over anhydrous $MgSO_4$. Remaining liquid crystallized in CCl_4 in the freezer (-18°C). Anal: calcd. for $C_{13}H_{23}NO_4$ C, 60.70; H, 8.94; N, 5.44; Found: C, 60.93; H, 8.76; N, 5.23. NMR (CCl_4 (ppm)): 5.25 (α-proton), 4.57 (q, α-proton), 3.95 (m, ketal ring protons), 2.6-1.0 (m, ring protons), 0.92 (d, t-bu protons).

SPECTRA

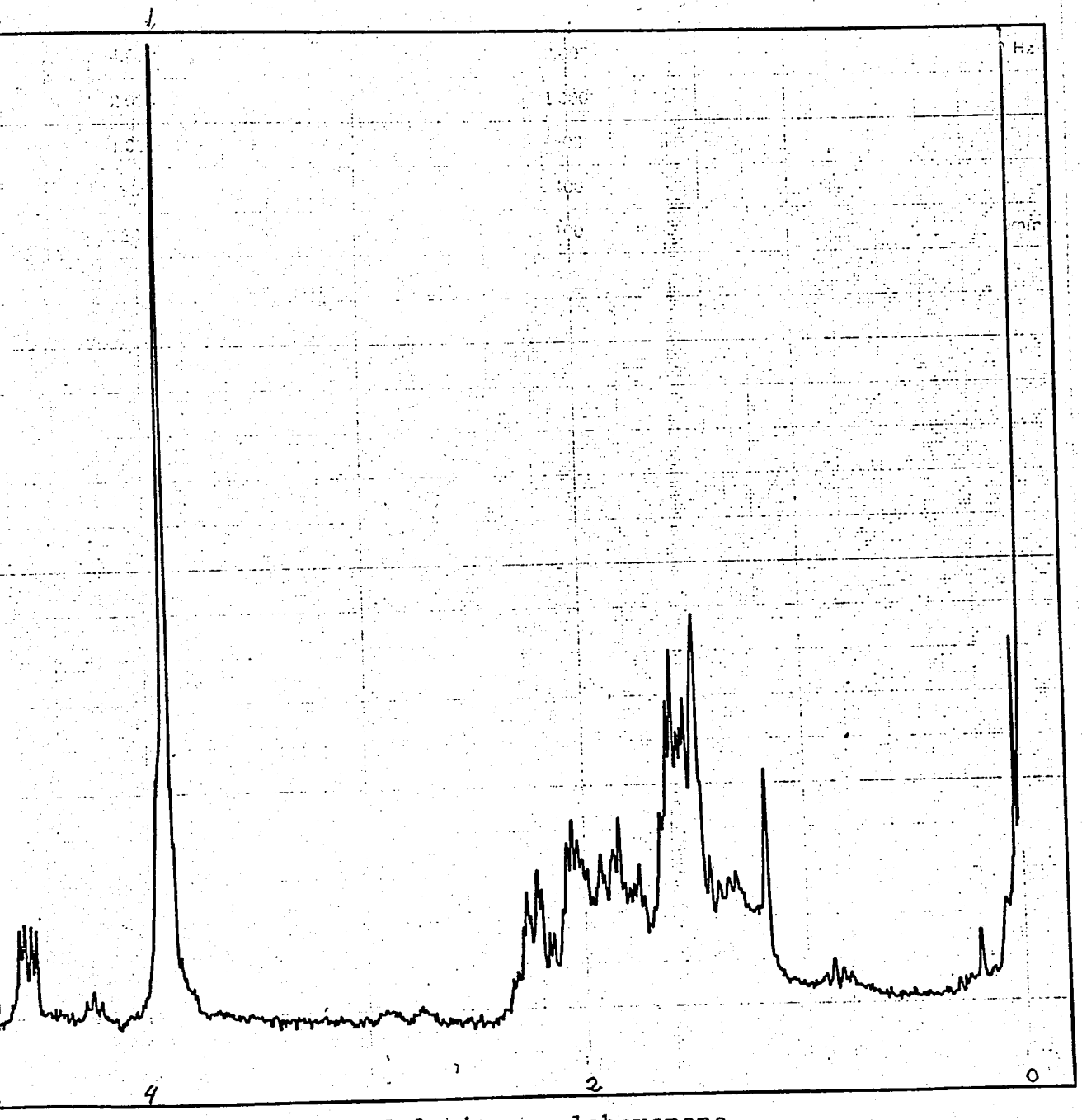

Ethylene Ketal of 2-nitrocyclohexanone

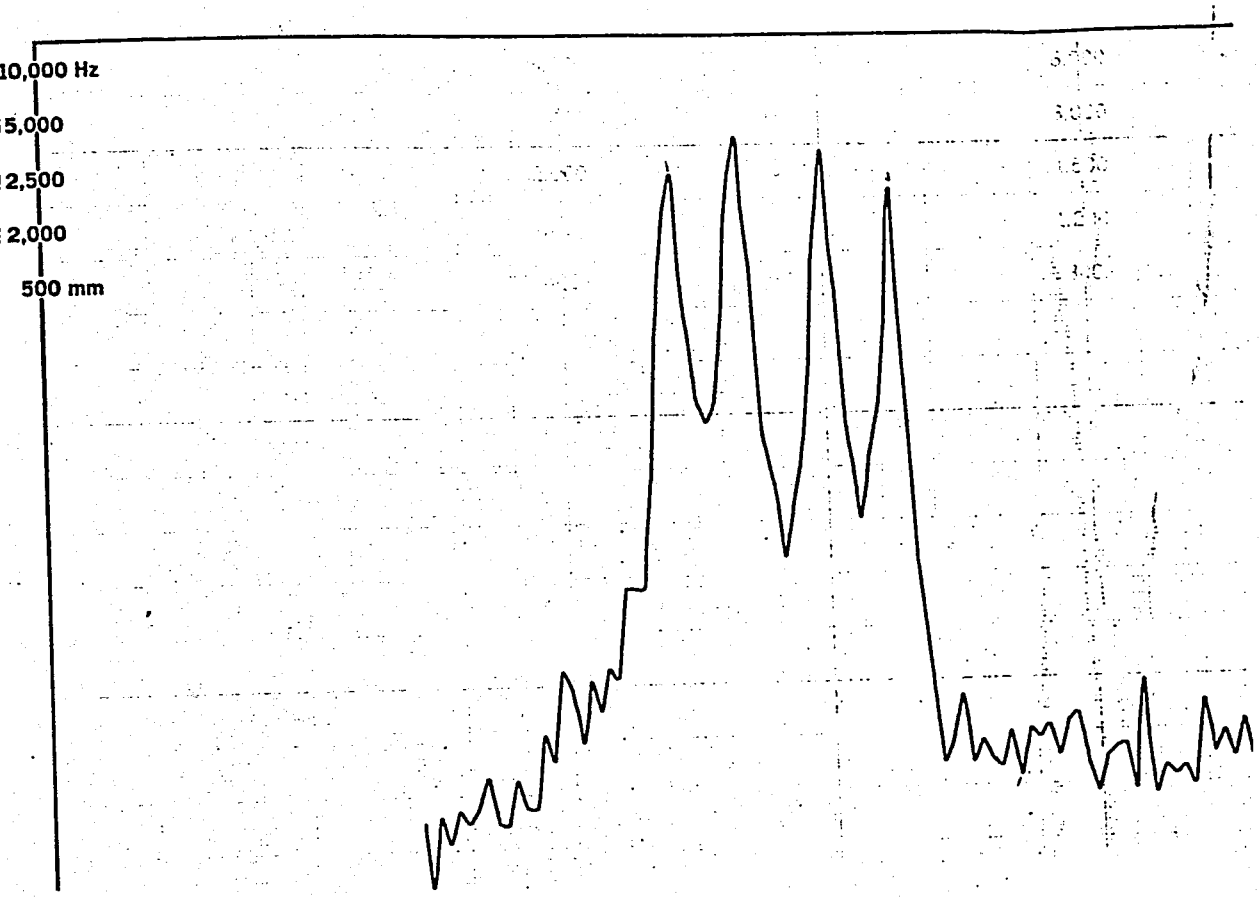

Ethylene Ketal of 2-nitrocyclohexanone
α-proton enlarged

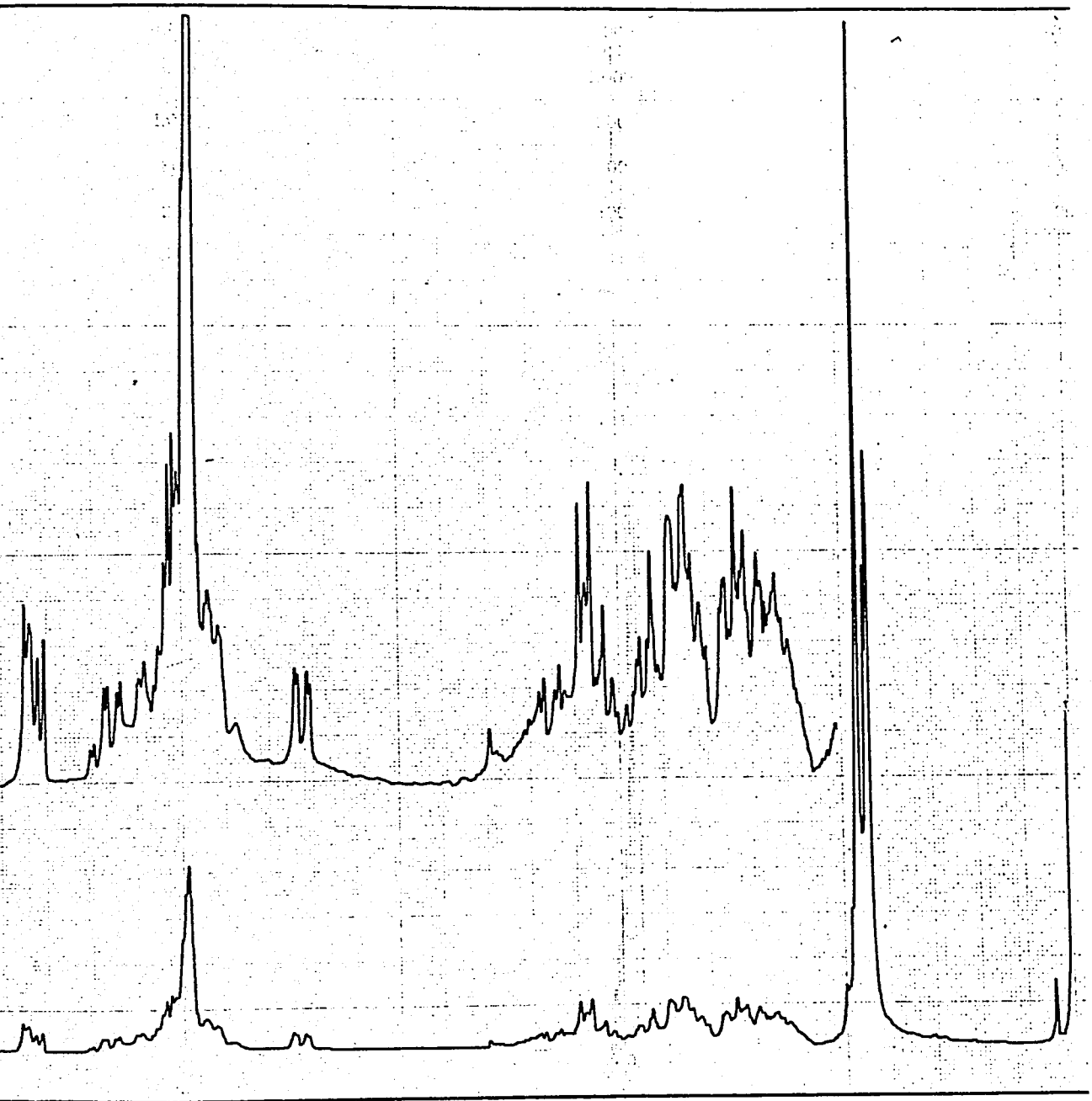

Ethylene Ketal of 4-t-butyl-2-nitrocyclohexanone

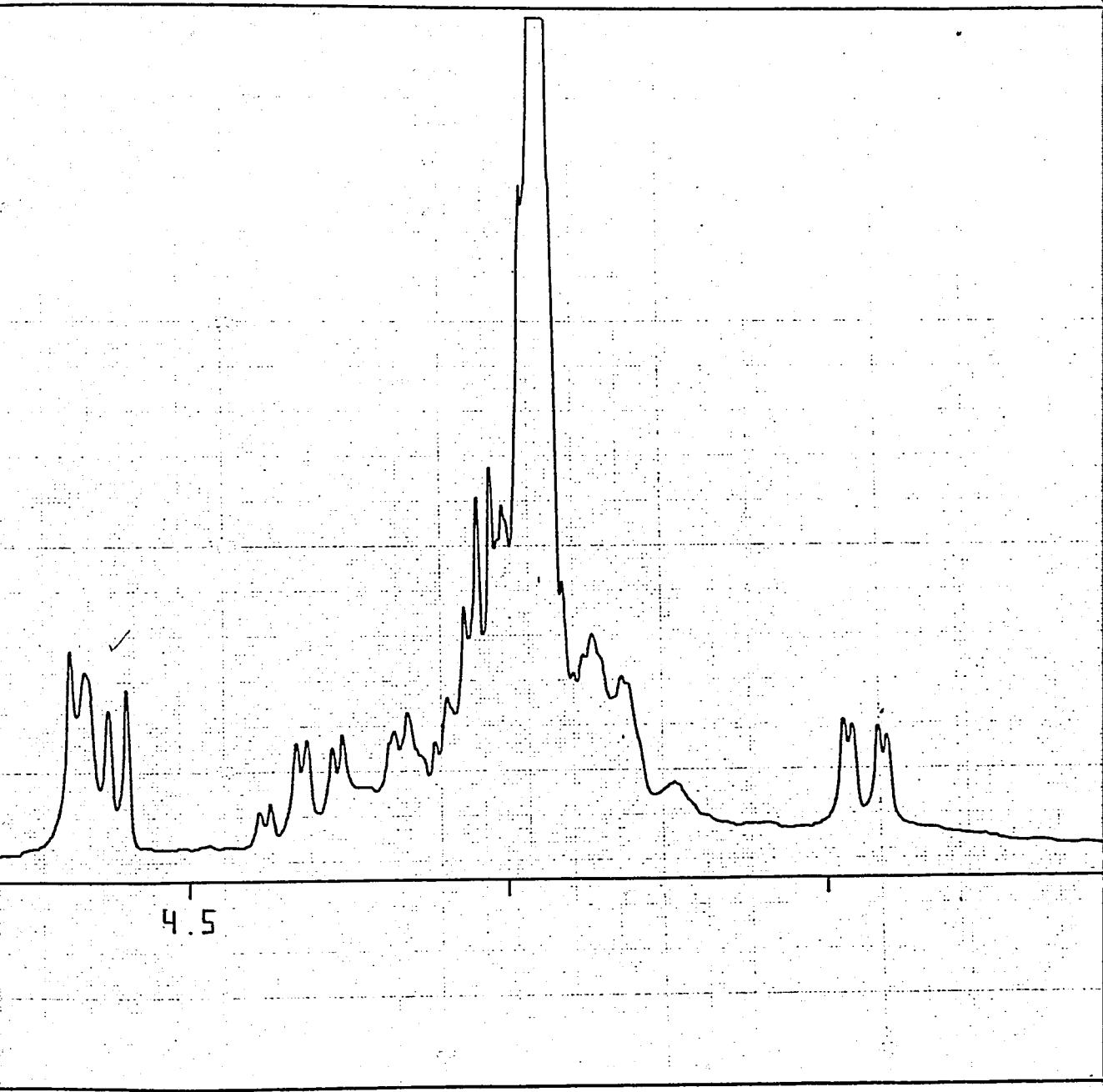

Ethylene Ketal of 4-t-butyl-2-nitrocyclohexanone
Width 691 Hz

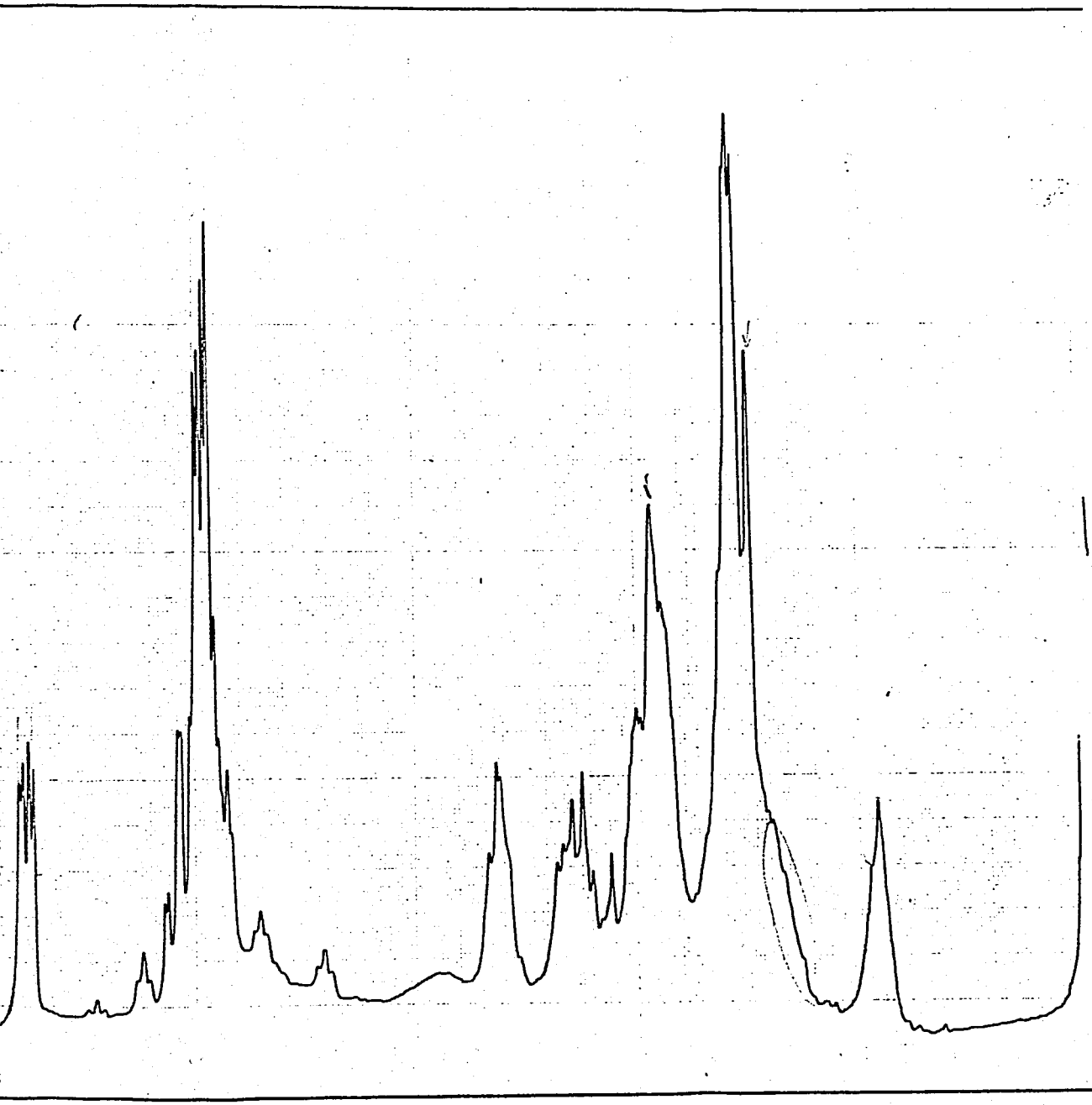

Propylene Ketal of 2-nitrocyclohexanone

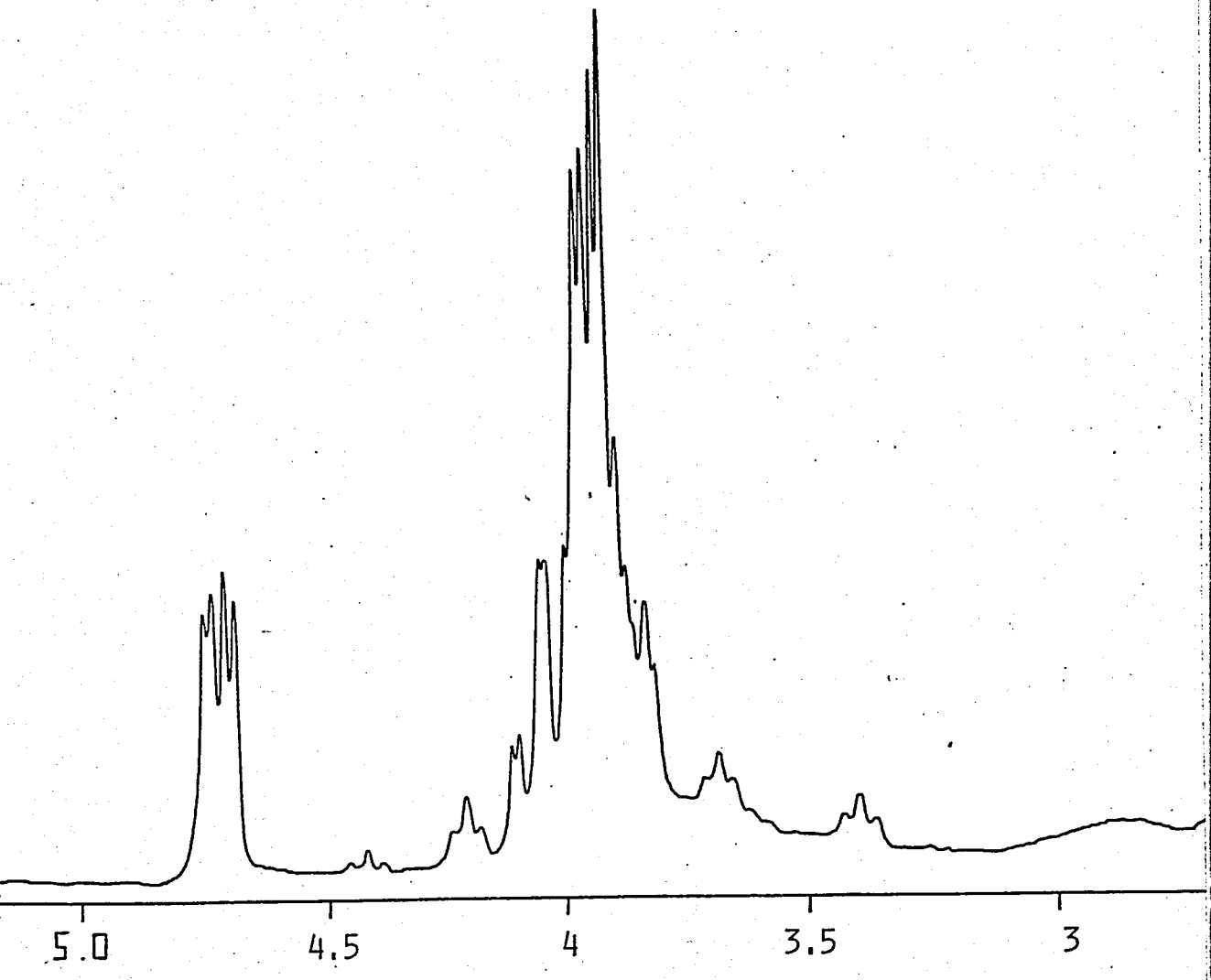

Propylene Ketal of 2-nitrocyclohexanone
Width 979.1 Hz

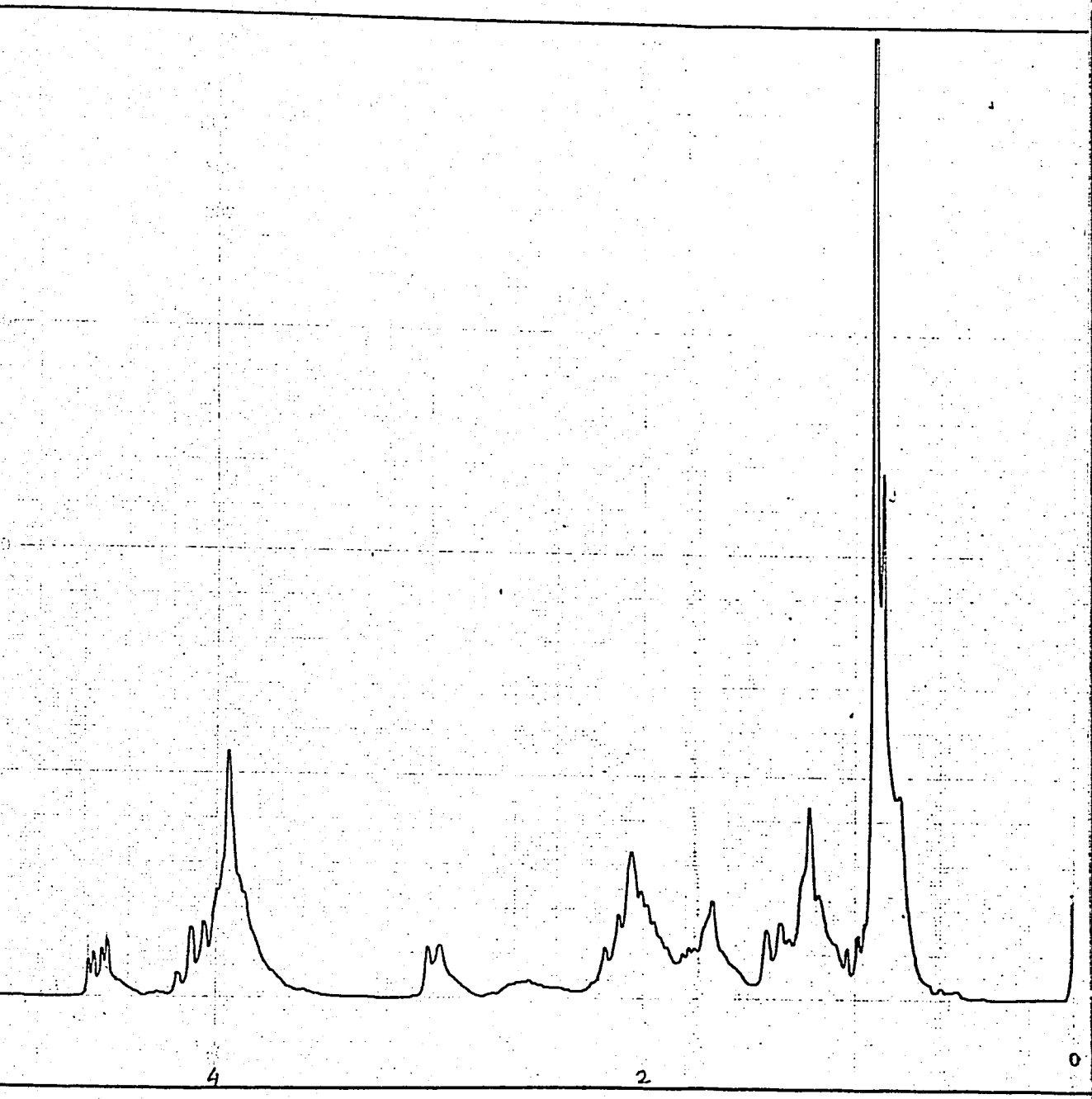

Propylene Ketal of 4-t-butyl 2-nitrocyclohexanone

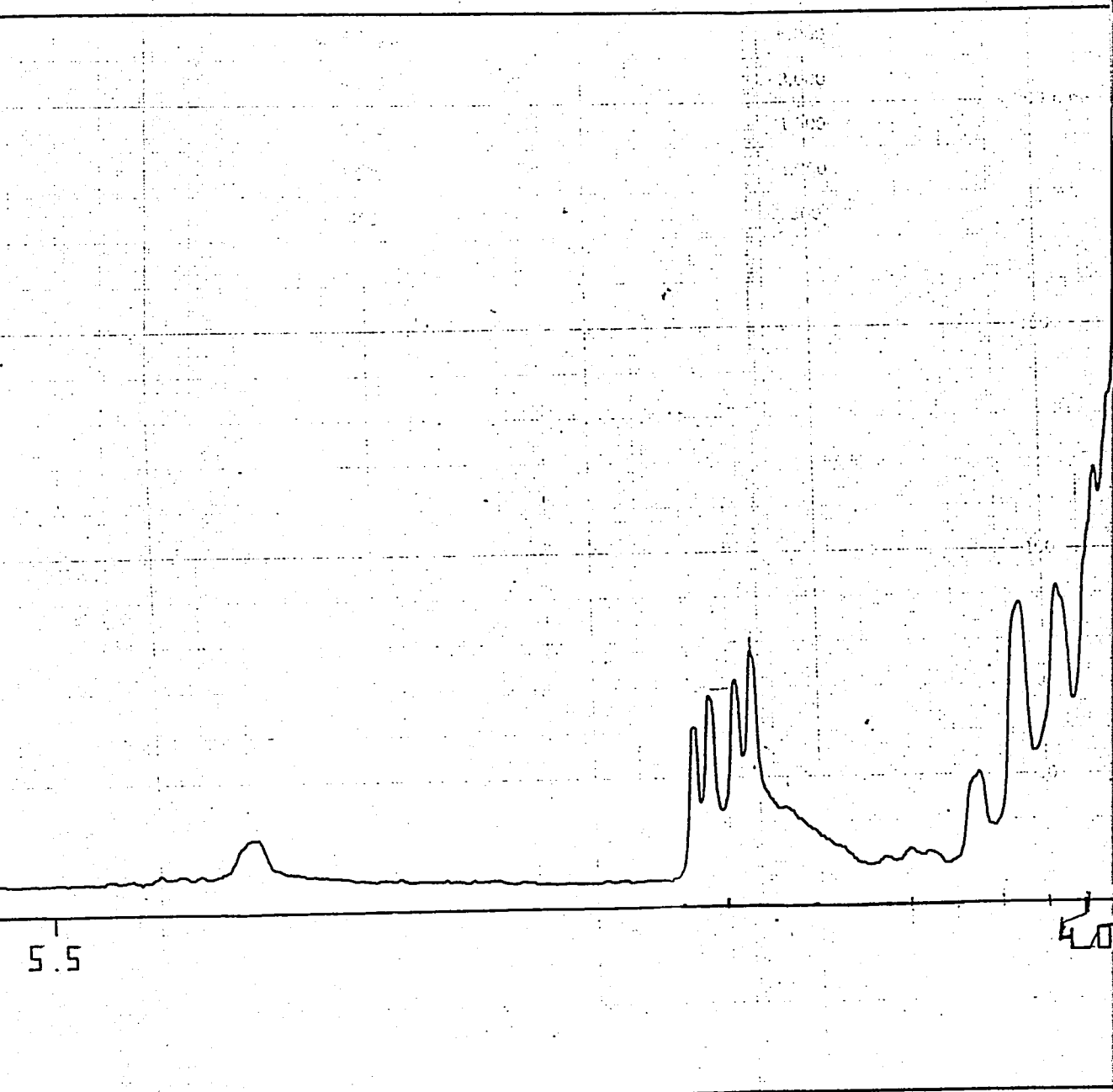

Propylene Ketal of 4-t-butyl 2-nitrocyclohexanone
α-protons enlarged

REFERENCES

1- Hurthocese, Moss and Sales, Chem. Soc. London. Annual Reports B (1978), p.23.

2- ref. 1, p.24.

3- J.B.Hendrickson, JACS, 83, 4537-47 (1961).

4- ref. 3, pg.27.

5- A.Y.Meyer, N.L.Allinger and Y.Yuh, Israel Journal of Chemistry, 20, 57-64 (1980).

6- ref. 5.

7- U.Burket, Tetrahedron, 35, 209-212 (1979).

8- N.L.Allinger, and D.Y.Chung, JACS, 98, 6798 (1976).

9- U.Burkert, Tetrahedron, 35, 691-695 (1979).

10- ref. 7.

11- N.L.Allinger, S.M.M.Chang, D.H.Glaser and H.Hönig, Israel Journal of Chemistry, 20, 51-56 (1980).

12- ref. 5.

13- Elicl, Alinger, Angyal, Marrison, Conformational Analysis Interscience, New York 1966.

14- ref. 13.

15- Steric Effects in Org. Chem ed. M.S.Newman, John Wiley and Sons Inc. New York, N.Y. 1965, Chapter 12.

16- ref. 13, p.448.

17- ref. 13, p.7-8.

18- Terrell,L.Hill, J. of Chem. Phy., 16, 399 (1948).

19- S.Binzet, Ph. D. Thesis (1980).

20- ref. 13, p.462.

21- Mursakulov, Guseinov, Kasumov, Zefirov, Samoshin and Chalenko, Tetrahedron 38, 2213-2220 (1982).

22- ref. 11.

23- ref. 11.

24- ref. 7.

25- ref. 8.

26- ref. 11.

27- ref. 13, pg.14.

28- ref. 13, pg.14

29- ref. 3.

30- ref. 3 and measurement.

31- ref. 13.

32- ref. 19.

33- ref. 3.

34- Abraham, Banks, Eliel, Hoter, Kaloustian, JACS, 94, 1913 (1972).

35- E.Juaristi, J. Clem. Ed., 56, 438 (1979).

36- ref. 13, p.447.

37- ref. 19.

38- ref. 18.

39- ref. 13.

40- L.J.Collins and D.N.Kirk, Tetrahedron Letters, 18, 1547-1550 (1970).

41- ref. 19.

42- ref. 11.

43- ref. 21.

44- I.G.Mursakulov, E.A.Ramazanov, V.V.Samoshin, N.S.Zefinov and E.L.Eliel, Zh. Org. Khim, 15, 2415 (1975). Mursahulov, Ramazanov, Gusenov, Zefirov, Sanoshin and Eliel, Tetrahedron 36, 1885 (1980).

45- ref. 19, pg.18-19.

46- ref. 19.

47- V.Sebüktekin, Ph.D. Thesis, 1980.

48- Franklin and Feltkamp. Angew. Chem. Internat. Edit. 4, 774 (1965).

49- H.Özbal, Ph. D. Thesis, 1971.

50- H.Özbal, Ph. D. Thesis, 1971.

51- S.Winstein, N.J.Holness, JACS, 77, 5562 (1955).

52- ref. 48.

53- ref. 48, ref. 47, pg.25.

54- ref. 49, pg.69.

55- ref. 49, pg.69.

56- H.Özbal, Ph. D. Thesis, 1971.

57- H.Özbal, Ph. D. Thesis, 1971.

58- ref. 21.

59- ref. 34.

60- Zajac and Özbal, JACS, 45, 4154-4157 (1980).

61- Zefirov, Samoshin, Subbotin, Baranekov and Wolfe, Tetrahedron, 34, 2953 (1978).

62- T.Varnalı, M.S. Thesis, 1982.

63- T.Varnalı, M.S. Thesis, 1982.